THE TYPE Ia SUPERNOVA 1989B IN NGC 3627 (M66)

LISA A. WELLS,[1] M. M. PHILLIPS, NICHOLAS B. SUNTZEFF,[2] S. R. HEATHCOTE, MARIO HAMUY, M. NAVARRETE, M. FERNANDEZ, W. G. WELLER,[3] AND R. A. SCHOMMER

Cerro Tololo Inter-American Observatory,[4] National Optical Astronomy Observatories, Casilla 603, La Serena, Chile
Electronic mail: lwells@as.arizona.edu, mphillips@noao.edu

ROBERT. P. KIRSHNER, BRUNO LEIBUNDGUT,[5] AND S. P. WILLNER

Harvard-Smithsonian Center for Astrophysics, 60 Garden Street, Cambridge, Massachusetts 02138

R. F. PELETIER

RGO, Apartado 321, 38700 Santa Cruz de la Palma, Tenerife/Canarias, Spain

ERIC M. SCHLEGEL[6]

Goddard Space Flight Center, Laboratory of High Energy Astrophysics, Code 668, Greenbelt, Maryland 20771

J. CRAIG WHEELER[7] AND ROBERT P. HARKNESS

Department of Astronomy, University of Texas, Austin, Texas 78712

DAVID J. BELL[8]

Department of Astronomy, University of Illinois, 1002 W. Green St., Urbana, Illinois 60801

JAYMIE M. MATTHEWS[8]

Department of Geophysics and Astronomy, University of British Columbia, Vancouver V6T 1Z4, Canada

ALEXEI V. FILIPPENKO,[9] JOSEPH C. SHIELDS,[10] AND MICHAEL W. RICHMOND[11]

Department of Astronomy, and Center for Particle Astrophysics, University of California, Berkeley, California 94720

D. JEWITT[2]

Institute for Astronomy, University of Hawaii, 2680 Woodlawn Drive, Honolulu, Hawaii 96822

JANE LUU[2]

Department of Physics, Stanford University, Varian Building, Stanford, California 94305-4060

HIEN D. TRAN

Caltech, Astronomy 105-24, Pasadena, California 91125

P. N. APPLETON

Astronomy Program, Department of Physics, 12 Physics Building, Iowa State University, Ames, Iowa 50011

E. I. ROBSON

School of Physics and Astronomy, Lancashire Polytechnic, Preston PR1 2TQ, United Kingdom

J. ANTHONY TYSON[8]

AT&T Bell Laboratories, Murray Hill, New Jersey 07974

P. GUHATHAKURTA[8]

Princeton University Observatory, Princeton, New Jersey 08540

JO ANN EDER[8]

National Astronomy and Ionosphere Center,[12] Arecibo Observatory, P.O. Box 995, Arecibo, Puerto Rico 00613

HOWARD E. BOND[8] AND MICHAEL POTTER[8]

Space Telescope Science Institute, 3700 San Martin Drive, Baltimore, Maryland 21218

S. VEILLEUX AND ALAIN C. PORTER[13]

Kitt Peak National Observatory,[14] National Optical Astronomy Observatories, P.O. Box 26732, Tucson, Arizona 85726

 0004-6256/94/108(6)/2233/18/$0.90

ROBERTA M. HUMPHREYS[8]
Department of Astronomy, University of Minnesota, 116 Church Street S. E., Minneapolis, Minnesota 55455

KENNETH A. JANES[8]
Department of Astronomy, Boston University, 725 Commonwealth Ave., Boston, Massachusetts 02215

T. B. WILLIAMS[8]
Department of Physics and Astronomy, Rutgers University, P.O. Box 849, Serin Physics Laboratory, Piscataway, New Jersey 08854

EDGARDO COSTA[8] AND MARÍA TERESA RUÍZ[8]
Departamento de Astronomia, Universidad de Chile, Casilla 36-D, Santiago, Chile

J. T. LEE[8]
Department of Astronomy, Yale University, P.O. Box 6666, New Haven, Connecticut 06511

J. H. LUTZ[8]
Program in Astronomy, Washington State University, Pullman, Washington 99164-2930

R. MICHAEL RICH[8]
Department of Astronomy, Box 52, Pupin Hall, 538 West 120th St., Columbia University, New York, New York 10027

P. FRANK WINKLER[8]
Department of Physics, Middlebury College, Middlebury, Vermont 05753

NEIL D. TYSON[8]
Department of Astrophysical Sciences, Princeton University, Princeton, New Jersey 08540
Received 1994 May 10; revised 1994 July 15

ABSTRACT

We report extensive optical photometry and spectroscopy of the Type Ia supernova 1989B. Maximum light in B occurred approximately seven days after discovery on JD 2447565.3±1.0 (1989 February 7.8±1.0) at a magnitude of 12.34±0.05. The *UBV* light curves of this supernova were very similar to those of other well observed Type Ia events such as SN 1981B and SN 1980N. From a comparison of the *UBVRIJHK* photometry, we derive an extinction for SN 1989B of $E(B-V)=0.37\pm0.03$ mags relative to the unobscured Type Ia SN 1980N. The properties of the dust responsible for the reddening of SN 1989B appear to have been similar to those of normal dust in the Milky Way. In particular, we find no evidence for an unusually low value of the ratio of the total to selective absorption. We derive a distance modulus of $\Delta\mu_0=-1.62\pm0.03$ mag relative to the Type Ia SN 1980N. We present optical spectra which provide essentially continuous coverage of the spectral evolution of SN 1989B over the first month following *B* maximum. These data show the transition from the maximum-light spectrum, in which lines of elements such as Ca, Si, S, Mg, and O are most prominent, to the Fe-dominated spectrum observed a few weeks after maximum. This transition occurred quite smoothly over a two-week period following *B* maximum. Comparison of the spectra of SN 1989B with data for two other well observed Type Ia supernovae—1981B and 1986G—reveals subtle differences in the relative strengths of the S II and Si II absorption lines at maximum light. However, these differences disappeared within a week or so after maximum with the onset of the Fe-dominated phase.

---

[1]Current Address: University of Arizona, Steward Observatory, Tucson, Arizona 85721.
[2]Visiting Astronomer, Kitt Peak National Observatory, National Optical Astronomy Observatories, operated by the Association of Universities for Research in Astronomy, Inc., (AURA) under cooperative agreement with the National Science Foundation.
[3]Current Address: Gemini Project, 950 North Cherry Ave, Tucson, AZ 85726.
[4]Cerro Tololo Inter-American Observatory, National Optical Astronomy Observatories, operated by the Association of Universities for Research in Astronomy, Inc., (AURA) under cooperative agreement with the National Science Foundation.
[5]Current Address: ESO, Karl-Schwarzschild-Strasse 2, Garching bei München, Germany.
[6]Research Scientist, Universities Space Research Association.
[7]AURA Visiting Professor, 1989–1990.
[8]Visiting Astronomer, Cerro Tololo Inter-American Observatory, National Optical Astronomy Observatories, operated by the Association of Universities for Research in Astronomy, Inc., (AURA) under cooperative agreement with the National Science Foundation.

[9]Presidential Young Investigator.
[10]Current Address: University of Arizona, Steward Observatory, Tucson, AZ 85721.
[11]Current Address: Department of Astrophysical Sciences, Princeton University, Princeton, NJ 08540.
[12]The Arecibo Observatory is part of the National Astronomy and Ionosphere Center. The NAIC is operated by Cornell University under a cooperative agreement with the National Science Foundation.
[13]Deceased, 10 October 1993.
[14]Kitt Peak National Observatory, National Optical Astronomy Observatories, operated by the Association of Universities for Research in Astronomy, Inc., (AURA) under cooperative agreement with the National Science Foundation.

1. INTRODUCTION

The supernova 1989B was discovered by Evans (1989) on January 30.5 UT in a bright spiral arm of the Sb(s)II.2 (Sandage & Tammann 1981) galaxy NGC 3627 (M66). Optical spectral observations reported by Cappellaro & Turatto (1989), Kirshner (1989), Suntzeff (1989), and Filippenko (1989) showed that SN 1989B was a Type Ia event (SN Ia), and pre-discovery images obtained by the Berkeley Automated Supernova Search (Marvin & Perlmutter 1989) suggested that maximum had not yet been reached. NGC 3627 is a member of the Leo trio of galaxies whose other members are NGC 3623 (M65) and NGC 3628. Surface photometry reveals clear evidence that NGC 3627 and NGC 3628 are interacting (Burkhead & Hutter 1981). SN 1989B is the second supernova to be discovered in NGC 3627, the first being the Type II plateau supernova 1973R (Ciatti & Rosino 1977) which reached a maximum brightness of $B\sim15$ mags.

Although many SNe Ia are discovered each year—the Asiago Supernova Catalog (Barbon *et al.* 1989) lists 60 confirmed Ia events in the 52 years leading up to 1989—few have been studied in detail. Recognizing the opportunity presented by the discovery of SN 1989B to remedy this situation, an extensive campaign of optical photometry and low-dispersion spectroscopy was immediately organized using the observational facilities of the Cerro Tololo Inter-American Observatory (CTIO). These data, along with complementary optical and infrared observations obtained at several northern hemisphere sites, are the subject of the present paper. Independent optical photometry and spectroscopy of SN 1989B has been previously presented by Bolte *et al.* (1989), Barbon *et al.* (1990, hereafter BBCRT), Tsvetkov *et al.* (1990, hereafter TKVBI), Prabhu & Krishnamurthi (1990), and Volkov (1991), and a near-infrared spectrum was published by Lynch *et al.* (1990).

Details of the data acquisition and reduction are given in Sec. 2. In Sec. 3, the $UBV(RI)_{KC}$ light curves are presented along with the extensive set of optical spectra obtained. We also combine the light curves with two epochs of *JHK* photometry to estimate the extinction and relative distance modulus of SN 1989B with respect to the unobscured Type Ia SN 1980N. Finally, in Sec. 4, we discuss the implications of our observations, which provide the most complete record yet obtained of the spectral and photometric evolution of a Type Ia supernova.

2. DATA ACQUISITION AND REDUCTION

2.1 CCD Photometry

Broadband $UBV(RI)_{KC}$ images of SN 1989B were obtained using CCD detectors on the CTIO 4.0 m and 0.91 m telescopes beginning several days before maximum and continuing for slightly more than 500 days. Information pertaining to these data is given in Table 1. The observations with the 4.0 m telescope were made at the $f/2.66$ prime focus using a TI 800×800 CCD (0.29 arcsec pixel^{-1}); the 0.9 m images were taken at the $f/13.5$ Cassegrain focus using a TI 800×800 (0.25 arcsec pixel^{-1}) or Tektronix 512×512 CCD (0.45 arcsec pixel^{-1}). Whenever possible, the same set of filters was used. The image calibrations, aperture photometry, and transformation to standard magnitudes were carried out at the CTIO La Serena headquarters using IRAF.[15]

Aperture photometry of the supernova was performed differentially with respect to the field stars listed in Table 2 which, except for Star 5, are shown in Fig. 1 [Plate 83]. These stars were calibrated from observations of Graham (1982) and Landolt (1983) standards obtained with the 0.9 m telescope on photometric nights between 1989 February 15–23. The resulting magnitudes and estimated errors are listed in Table 2. Also given in Table 2 are photoelectric *B* and *V* measurements of the field star 5 (also known as star A, see Ciatti & Rosino 1977) obtained with the 1.0 m telescope on four nights in the interval 1989 February 10–17. Photometry in *B* and *V* for most of these local standard stars has been previously published by Ciatti & Rosino (1977), BBCRT, and TKVBI, with the interagreement generally good to within the quoted errors, 0.02–0.03 mag. A large discrepancy found in the final magnitude for star 1 together with its very red color aroused suspicion that this star is variable and thus it was not used in the final analysis. Star 5 was not employed for the CCD photometry reductions since it often was not included in the relatively small field of the CCD detector. Hence, the final supernova CCD photometry is based on measurements made with respect to stars 2, 3, and 4.

Due to the location of SN 1989B in a bright spiral arm of NGC 3627, contamination of the photometry by the background galaxy light was a serious concern. To correct for this problem, we employed the same stellar aperture (radius =7.41 arcsec) and sky annulus (inner radius=7.41 arcsec, outer radius=12.35 arcsec) for the early measurements with aperture corrections as the SN faded. A final background correction was calculated using images taken approximately 1.5 years after maximum under good seeing conditions at the 4.0 m telescope when the supernova had faded beyond detection. For the same stellar aperture and sky annulus centered on the position of the supernova, we measured the following magnitudes for the background galaxy light:

[15]IRAF is distributed by the National Optical Astronomy Observatories, which is operated by the Association of Universities for Research in Astronomy, Inc., under contract to the National Science Foundation.

TABLE 1. Log of *UBVRI* CCD photometry.

U.T. Date	Julian Date	Telescope	Observer	Filters
1989 Feb. 4.29	2447561.79	CTIO 4.0-m	J Tyson/Guhathakurta	UR
1989 Feb. 4.36	2447561.86	CTIO 0.91-m	Lee	UBV
1989 Feb. 5.29	2447562.79	CTIO 4.0-m	J Tyson/Guhathakurta	UR
1989 Feb. 5.31	2447562.81	CTIO 0.91-m	Hamuy	BVRI
1989 Feb. 6.29	2447563.79	CTIO 4.0-m	J Tyson/Guhathakurta	UR
1989 Feb. 7.28	2447564.78	CTIO 4.0-m	J Tyson/Guhathakurta	UR
1989 Feb. 8.29	2447565.79	CTIO 4.0-m	J Tyson/Guhathakurta	UR
1989 Feb. 9.30	2447566.80	CTIO 4.0-m	Navarrete	UBVRI
1989 Feb. 10.35	2447567.85	CTIO 0.91-m	Janes	UBVRI
1989 Feb. 11.40	2447568.90	CTIO 4.0-m	Winkler	B
1989 Feb. 12.30	2447569.80	CTIO 0.91-m	Janes	UBVI
1989 Feb. 14.25	2447571.75	CTIO 0.91-m	Phillips	UBVRI
1989 Feb. 15.25	2447572.75	CTIO 0.91-m	Suntzeff	UBVRI
1989 Feb. 16.29	2447573.79	CTIO 0.91-m	Heathcote	UBVRI
1989 Feb. 17.27	2447574.77	CTIO 0.91-m	Wells	UBVRI
1989 Feb. 18.27	2447575.77	CTIO 0.91-m	Wells	UBVRI
1989 Feb. 19.28	2447576.78	CTIO 0.91-m	Wells	UBVRI
1989 Feb. 20.26	2447577.76	CTIO 0.91-m	Wells	UBVRI
1989 Feb. 21.22	2447578.72	CTIO 0.91-m	Wells	UBVRI
1989 Feb. 24.18	2447581.68	CTIO 0.91-m	Weller	UBVRI
1989 Feb. 25.25	2447582.75	CTIO 0.91-m	Potter	UBVR
1989 Feb. 27.22	2447584.72	CTIO 0.91-m	Potter	UBVR
1989 Feb. 28.26	2447585.76	CTIO 0.91-m	Potter	UBVR
1989 Mar. 3.20	2447588.70	CTIO 0.91-m	Potter	UBVR
1989 Mar. 5.22	2447590.72	CTIO 0.91-m	Eder	BVR
1989 Mar. 6.17	2447591.67	CTIO 0.91-m	Eder	BVR
1989 Mar. 7.23	2447592.73	CTIO 0.91-m	Eder	BVR
1989 Mar. 8.18	2447593.68	CTIO 0.91-m	Eder	BVR
1989 Mar. 10.22	2447595.72	CTIO 0.91-m	Eder	BVR
1989 Mar. 14.22	2447599.72	CTIO 4.0-m	Suntzeff	UBVRI
1989 Mar. 15.25	2447600.75	CTIO 0.91-m	Suntzeff	UBVRI
1989 Mar. 27.21	2447612.71	CTIO 0.91-m	Williams	BVRI
1989 Mar. 29.17	2447614.67	CTIO 0.91-m	Phillips	UBVRI
1989 Mar. 30.17	2447615.67	CTIO 0.91-m	Suntzeff	UBVRI
1989 Apr. 18.14	2447634.64	CTIO 0.91-m	Suntzeff	UBVRI
1989 Apr. 23.11	2447639.61	CTIO 0.91-m	Suntzeff	UBVRI
1989 Apr. 29.11	2447645.61	CTIO 4.0-m	Navarrete	UBVRI
1989 May 12.02	2447658.52	CTIO 0.91-m	Navarrete	BV
1989 May 23.06	2447669.56	CTIO 0.91-m	Suntzeff	UBVRI
1989 May 31.10	2447677.60	CTIO 0.91-m	Bond	BVRI
1989 Jun. 5.01	2447682.51	CTIO 0.91-m	Rich/N Tyson	UBVRI
1989 Jun. 16.06	2447693.56	CTIO 0.91-m	Navarrete	UBVRI
1989 Jun. 18.03	2447695.53	CTIO 0.91-m	Navarrete	UBVRI
1989 Dec. 12.33	2447872.83	CTIO 0.91-m	Suntzeff	BVRI
1989 Dec. 16.44	2447876.94	CTIO 0.91-m	Navarrete	VR
1990 Jan. 5.31	2447896.81	CTIO 0.91-m	Wells	UBVRI
1990 Jan. 25.29	2447916.79	CTIO 0.91-m	Wells	BVR
1990 Mar. 19.18	2447969.68	CTIO 0.91-m	Schommer	BVRI
1990 May 2.06	2448013.56	CTIO 0.91-m	Wells	BV
1990 Jun. 29.03	2448071.53	CTIO 4.0-m	Navarrete	UBVRI

$U=16.88\pm0.06$, $B=17.10\pm0.08$, $V=16.45\pm0.04$, $R=15.60\pm0.06$, and $I=14.68\pm0.04$. The B and V values were compared with photometry of images taken in 1990 May at the 0.9 m under average seeing conditions showing agreement within the quoted uncertainties above. The resulting corrections to the supernova photometry in B were quite small (0.01 mag) near maximum, but steadily grew to a value of 0.8 mag over the following year. As a test of the effectiveness of this correction procedure, we carried out independent measurements for two nights, one in 1989 April and the other in 1989 December, by fitting a point spread function (PSF) to the supernova image using the program DoPhot (Schechter *et al.* 1993). This method, which assumes that the underlying background light can be approximated by a linear intensity variation across the PSF, gave results which were consistent with the corrected aperture photometry to well within the errors of both methods.

TABLE 2. *UBVRI* CCD photometry for local standards.

Star	BBCRT*	V	U-B	B-V	V-R	R-I
1	1	9.79(.013)	1.01(.010)	1.11(.017)	0.58(.011)	0.48(.016)
2	5	13.17(.027)	-0.06(.038)	0.55(.030)	0.34(.016)	0.33(.028)
3		16.20(.031)		0.59(.032)		
4	f	15.94(.025)	0.17(.033)	0.59(.030)	0.33(.031)	0.41(.032)
5	A	13.64(.031)		0.78(.032)		

*Naming convention of Barbon et al. (1990).

TABLE 3. *UBVRI* CCD photometry.

Julian Date	U	B	V	R	I
2447561.79	12.32(.06)			11.82(.06)	
2447561.86			12.09(.06)		
2447562.79	12.45(.07)			11.83(.07)	
2447562.81		12.36(.08)	12.02(.04)	11.85(.07)	11.70(.07)
2447563.79	12.47(.07)			11.89(.07)	
2447564.78	12.46(.07)			11.86(.07)	
2447565.79	12.56(.07)			11.90(.07)	
2447566.80	12.55(.06)	12.41(.08)	12.02(.07)	11.83(.06)	11.88(.10)
2447567.85	12.59(.06)	12.45(.08)	11.99(.04)	11.76(.13)	11.86(.15)
2447568.90		12.46(.08)			
2447569.80	12.80(.06)	12.52(.08)	12.02(.04)		11.90(.07)
2447571.75	12.98(.06)	12.65(.08)	12.08(.12)	11.92(.06)	12.00(.04)
2447572.75	13.09(.06)	12.73(.08)	12.08(.07)	11.92(.06)	11.99(.10)
2447573.79	13.10(.06)	12.75(.14)	12.14(.05)	11.97(.06)	12.03(.04)
2447574.77	13.26(.06)	12.90(.08)	12.17(.14)	12.08(.06)	12.15(.04)
2447575.77	13.42(.06)	13.02(.08)	12.25(.08)	12.16(.11)	12.18(.09)
2447576.78	13.64(.06)	13.18(.08)	12.34(.04)	12.21(.06)	12.21(.06)
2447577.76	13.81(.06)	13.28(.10)	12.41(.07)	12.24(.07)	12.19(.07)
2447578.72	14.00(.06)	13.41(.08)	12.49(.05)	12.23(.06)	12.28(.08)
2447581.68	14.48(.05)	13.74(.12)	12.65(.04)	12.35(.06)	12.16(.04)
2447582.75	14.54(.06)	13.95(.09)	12.68(.04)	12.26(.06)	
2447584.72	14.87(.06)	14.11(.08)	12.87(.04)	12.48(.06)	
2447585.76	14.96(.15)	14.27(.08)	12.83(.08)	12.47(.06)	
2447588.70	15.30(.06)	14.57(.08)	13.12(.04)	12.60(.06)	
2447590.72		14.79(.08)	13.05(.04)	12.57(.06)	
2447591.67		14.83(.08)	13.20(.04)	12.65(.06)	
2447592.73		15.02(.08)	13.28(.05)	12.75(.06)	
2447593.68		15.09(.10)	13.33(.04)	12.82(.08)	
2447595.72		15.26(.08)	13.46(.04)	12.98(.06)	
2447599.72	15.77(.19)	15.20(.09)	13.71(.08)	13.27(.09)	12.70(.13)
2447600.75	15.51(.56)	15.24(.36)	13.97(.12)	13.40(.06)	12.57(.33)
2447612.71		15.59(.10)	14.23(.10)	13.82(.08)	
2447614.67	16.39(.43)	15.73(.33)	14.27(.24)	13.85(.08)	13.09(.24)
2447615.67	16.54(.35)	15.62(.27)	14.25(.20)	13.88(.13)	13.49(.20)
2447634.64	16.33(.12)	16.03(.12)	14.95(.41)	14.54(.27)	14.82(.55)
2447639.61	16.55(.20)	15.89(.10)	14.93(.13)	14.63(.10)	14.97(.37)
2447645.61	16.81(.39)	15.86(.13)	14.89(.09)	14.89(.12)	14.63(.19)
2447658.52		16.31(.43)	15.11(.33)		
2447669.56	16.91(.38)	16.58(.54)	15.65(.11)	15.58(.22)	15.80(.33)
2447677.60		16.37(.10)	15.80(.20)	15.55(.16)	16.33(.50)
2447682.51	18.27(.52)	16.72(.19)	16.03(.19)	15.98(.18)	16.43(.47)
2447693.56	18.51(.39)	16.74(.20)	16.12(.15)	16.30(.22)	16.61(.45)
2447695.53	18.24(.41)	16.87(.13)	16.24(.19)	16.28(.16)	16.50(.36)
2447872.83		18.78(.44)	18.38(.34)	18.51(.36)	17.98(.43)
2447896.81			18.44(.21)		
2447916.79		19.24(.60)	18.64(.26)		

Final results of the background-corrected CCD photometry of SN 1989B are given in Table 3. The errors in the initial magnitudes of the supernova plus galaxy and the galaxy background were summed in quadrature to produce the final errors in brackets quoted in Table 3.

2.2 Photoelectric Photometry

Photoelectric photometry of SN 1989B was obtained on several nights around maximum with a single-channel photometer and standard B and V filters using the CTIO 1.0 m, 0.6 m, and 0.4 m telescopes. Information relevant to these observations is listed in Table 4. The aperture sizes employed ranged from 12 to 19.5 arcsec, and special care was taken to obtain sky measurements well away from NGC 3627. The data were reduced and calibrated via observations of Landolt (1983) standard stars and/or the local standard star 5 (see Table 2). Corrections for the background galaxy light included in the supernova measurements were derived from

TABLE 4. Log of *BV* photoelectric photometry.

U.T. Date	Julian Date	Telescope	Observer
1989 Feb. 4.33	2447561.83	CTIO 0.41-m	Hamuy
1989 Feb. 8.31	2447565.81	CTIO 0.60-m	Matthews
1989 Feb. 9.35	2447566.85	CTIO 0.60-m	Matthews
1989 Feb. 10.27	2447567.77	CTIO 0.41-m	Hamuy
1989 Feb. 10.27	2447567.77	CTIO 1.0-m	Bell
1989 Feb. 10.36	2247567.86	CTIO 0.60-m	Matthews
1989 Feb. 11.33	2447568.83	CTIO 1.0-m	Bell
1989 Feb. 12.26	2447569.76	CTIO 0.41-m	Hamuy
1989 Feb. 12.26	2447569.76	CTIO 1.0-m	Bell
1989 Feb. 12.36	2447569.86	CTIO 0.60-m	Matthews
1989 Feb. 13.27	2447570.77	CTIO 1.0-m	Bell
1989 Feb. 13.37	2447570.87	CTIO 0.60-m	Matthews
1989 Feb. 14.26	2447571.76	CTIO 1.0-m	Bell
1989 Feb. 14.34	2447571.84	CTIO 0.60-m	Matthews
1989 Feb. 15.26	2447572.76	CTIO 1.0-m	Bell
1989 Feb. 15.36	2447572.86	CTIO 0.60-m	Matthews
1989 Feb. 16.28	2447573.78	CTIO 1.0-m	Bell
1989 Feb. 16.37	2447573.87	CTIO 0.60-m	Matthews
1989 Feb. 17.27	2447574.77	CTIO 1.0-m	Bell
1989 Feb. 17.34	2447574.84	CTIO 0.60-m	Matthews
1989 Feb. 18.36	2447575.86	CTIO 0.60-m	Matthews
1989 Feb. 19.36	2447576.86	CTIO 0.60-m	Matthews
1989 Feb. 20.36	2447577.86	CTIO 0.60-m	Matthews
1989 Feb. 21.37	2447578.87	CTIO 0.60-m	Matthews
1989 Feb. 22.36	2447579.86	CTIO 0.60-m	Matthews

TABLE 5. *BV* photoelectric photometry.

Julian Date	B	V
2447561.83	12.48(.06)	12.25(.04)
2447565.81	12.29(.08)	11.83(.08)
2447566.85	12.41(.08)	11.92(.08)
2447567.77	12.34(.06)	12.06(.04)
2447567.77	12.48(.03)	11.99(.03)
2447567.86	12.38(.08)	11.96(.08)
2447568.83	12.50(.03)	12.00(.03)
2447569.76	12.46(.07)	12.08(.04)
2447569.76	12.55(.03)	12.02(.03)
2447569.86	12.54(.08)	11.99(.08)
2447570.77	12.62(.03)	12.04(.03)
2447570.87	12.58(.08)	11.99(.08)
2447571.76	12.70(.03)	12.09(.03)
2447571.84	12.66(.09)	12.05(.08)
2447572.76	12.77(.03)	12.11(.03)
2447572.86	12.76(.09)	12.12(.08)
2447573.78	12.87(.03)	12.17(.03)
2447573.87	12.87(.09)	12.15(.08)
2447574.77	12.97(.04)	12.23(.03)
2447574.84	12.96(.09)	12.20(.08)
2447575.86	13.10(.10)	12.29(.09)
2447576.86	13.35(.11)	12.38(.09)
2447577.86	13.36(.11)	12.49(.09)
2447578.87	13.62(.12)	12.51(.09)
2447579.86	13.72(.13)	12.69(.09)

the previously described CCD images obtained after the supernova had disappeared, although the exact method employed was somewhat distinct from the procedure described in Sec. *2.1*. In particular, a mean sky value determined from pixels in the CCD image lying well away from NGC 3627 was subtracted from the CCD data. The intensity of the background light of NGC 3627 centered on the position of the supernova and corresponding to each of the aperture radii employed for the photoelectric observations was then calculated from the sky-subtracted CCD images, and the results were used to correct the photoelectric data. The final background-corrected photoelectric photometry for SN 1989B is given in Table 5.

2.3 Infrared Photometry

Near-infrared images of SN 1989B in the *JHK* bands were obtained using the IRCAM InSb 62×58 pixel infrared array camera attached to the 3.8 m United Kingdom Infrared Telescope (UKIRT)[16] on the night of 1989 February 14.34 UT (JD 2447571.84). Photometric conditions were excellent with seeing around 1.5 arcsec. IRCAM was operated with a pixel scale of 1.24 arcsec pixel^{-1}, corresponding to an overall field of 74×70 arcsec. Total integration times at each position were 600 s in *K* and 400 s in *J* and *H*. Dark frames of equivalent integration time to the object frames were subtracted from all images and flatfielding was performed using adjacent sky frames of identical integration times as the on-source frames. A sequence of sky frames was median-filtered and normalized to produce a flat field image for each filter which was then divided into the object frames. Finally, a constant background level was removed from each frame and the observations were corrected for airmass using average extinction coefficients for UKIRT. Calibration was achieved via observations of the standard stars HD 44612 and GL 406 (Elias *et al.* 1982). Magnitudes for the supernova were measured using aperture photometry techniques, with the correction for the galaxy background calculated from an equivalent sized aperture placed on the spiral arm near the supernova. Final results for this night with the 3σ uncertainties are given in Table 6.

A second epoch of *JHK* photometry of SN 1989B was obtained on 1989 February 27.36 UT (JD 2447584.9) with the 0.6 m telescope of the F. L. Whipple Observatory on Mt. Hopkins. These observations were made with the SONIC infrared camera which also employed a 62×58 pixel InSb array with a pixel size of 3.55 arcsec. Two independent images of the supernova were obtained in each of *J* and *H* bands, and nine in *K* (180 s each in *J* and *H*, 30 s each in *K*). Two standard stars from Elias *et al.* (1982) were also observed—HD 44612 before the supernova observations and HD 129655 after. Each standard was observed four times in two different positions on the array. The SN images were generally characterized by a FWHM of 2 pixels or less. Instrumental magnitudes were measured for the SN after subtracting the galaxy background, with the latter calculated by determining the peak of the sky histogram between 3 and 6 pixels from the SN. The resulting magnitudes are listed in Table 6. The errors quoted in Table 6 are dominated by the uncertainty in the galaxy background correction for both nights.

[16]The United Kingdom Infrared Telescope is operated by the Royal Observatory, Edinburgh.

TABLE 6. Infrared photometry.

U.T. Date	Julian Date	Telescope	Observer	J	H	K
1989 Feb. 14.34	2447571.84	UKIRT	Appleton/Robson	12.80(.07)	12.40(.07)	12.20(.11)
1989 Feb. 27.36	2447584.86	Whipple 0.6-m	Willner	13.22(.05)	11.91(.05)	11.58(.10)

2.4 Optical Spectroscopy

Extensive optical spectroscopy of SN 1989B at resolutions ranging between 3 and 16 Å was obtained using the CTIO 4.0 m, 1.5 m, and 1.0 m telescopes, the KPNO 2.1 m telescope, the 3.0 m and 1.0 m telescopes at Lick Observatory, the 1.5 m telescope at the F. L. Whipple Observatory, and the Multiple Mirror Telescope (MMT). The majority of the spectra recorded over the first two months were acquired with the CTIO 1.0 m telescope Cassegrain spectrograph equipped with a "2D-Frutti," two-dimensional photon-counting detector. A "2D-Frutti" detector was employed for a single spectrum obtained with the CTIO 4.0 m telescope Cassegrain spectrograph, and the three observations made with the F. L. Whipple Observatory 1.5 m telescope were obtained with a photon-counting, intensified Reticon detector (the so-called "Z-Machine"). All other observations were carried out using CCD detectors. A log of the complete set of 52 spectra obtained is given in Table 7.

All of the optical spectra were reduced and calibrated using standard techniques. Wavelength calibrations were carried out via comparison lamp exposures taken at the position of the supernova. The spectra were corrected for atmospheric extinction using mean extinction curves for the different sites, and the final flux calibrations were derived from observations of one or more spectrophotometric standard stars (Stone & Baldwin 1983; Oke & Gunn 1983; Massey *et al.* 1988). The precision of the flux calibration for the spectra obtained at early epochs when SN 1989B was bright is generally good. However, as the supernova faded, the observations unavoidably suffered from increasing contamination by the background light of the parent galaxy. Hence, neither the absolute nor relative flux scales of the late-epoch spectra should be taken as reliable.

3. RESULTS

3.1 The Optical Light Curves

Figure 2(a) shows the *UBV* photometry of SN 1989B from Tables 3 and 5 plotted as a function of the Julian date. Included for comparison in this figure are Leibundgut's (1988) template *UBV* light curves for SNe Ia. To fit these curves to the data, we determined the time and the magnitude of maximum light for SN 1989B in the *B* and *V* filters by fitting a third-order polynomial to the photometry obtained over the first 20 days of observation. The results are listed in Table 8, where column (1) gives the time of maximum light, column (2) the magnitude at the time of maximum light, and column (3) the magnitude at the time of *B* maximum, $m(t_0^B)$. The errors given in this table represent the range of acceptable fits to the data. Within the accuracy of our measurements, the time difference between the *B* and *V* maxima is consistent with the value $t_0^V - t_0^B = 2$ days assumed by Leibundgut (1988). We thus fit the template light curves to the data in Fig. 2(a) by shifting the curves in unison along the abscissa (i.e., maintaining the time differences given by Leibundgut) to match the time of maximum light in the *B* filter, t_0^B. The vertical shift was accomplished independently for each filter by matching the observed magnitude of SN 1989B in that band at t_0^B.

The *R* and *I* light curves of SN 1989B, which are displayed in Fig. 2(b), are among the most extensive ever obtained for a SN Ia. Included for comparison in the same

TABLE 7. Log of spectroscopic observations.

U.T. Date	Julian Date	Telescope	Instrument	Observer
1989 Jan. 31.20	2447557.70	KPNO 2.1-m	Gold Camera	Suntzeff
1989 Jan. 31.30*	2447557.80	MMT	Red Channel	Wilkes
1989 Jan. 31.47*	2447557.97	Lick 3.0-m	CS/CCD	Veilleux/Tran
1989 Feb. 1.44	2447558.94	Whipple 1.5-m	Z-machine	Whipple Obs. Staff
1989 Feb. 3.55*	2447561.05	Whipple 1.5-m	Z-machine	Whipple Obs. Staff
1989 Feb. 4.30	2447561.80	CTIO 1.0-m	CS/2DF	Humphreys
1989 Feb. 4.30	2447561.80	CTIO 1.5-m	CS/CCD	Costa
1989 Feb. 4.42	2447561.92	KPNO 2.1-m	Gold Camera	Jewitt/Luu
1989 Feb. 4.55	2447562.05	Whipple 1.5-m	Z-machine	Whipple Obs. Staff
1989 Feb. 5.32	2447562.82	CTIO 1.0-m	CS/2DF	Humphreys
1989 Feb. 6.35*	2447563.85	CTIO 1.5-m	CS/CCD	Wells
1989 Feb. 7.39	2447564.89	KPNO 2.1-m	Gold Camera	Jewitt/Luu
1989 Feb. 8.32*	2447565.82	Whipple 1.5-m	Z-machine	Whipple Obs. Staff
1989 Feb. 10.31*	2447567.81	CTIO 1.0-m	CS/2DF	Hamuy
1989 Feb. 12.28*	2447569.78	CTIO 1.0-m	CS/2DF	Hamuy
1989 Feb. 14.29	2447571.79	CTIO 1.0-m	CS/2DF	Phillips
1989 Feb. 14.41	2447571.91	Whipple 1.5-m	Z-machine	Whipple Obs. Staff
1989 Feb. 15.45*	2447572.95	Lick 1.0-m	CS/CCD	Filippenko
1989 Feb. 16.30	2447573.80	CTIO 1.0-m	CS/2DF	Heathcote
1989 Feb. 18.29*	2447575.79	CTIO 1.0-m	CS/2DF	Wells
1989 Feb. 19.27	2447576.77	CTIO 1.0-m	CS/2DF	Wells
1989 Feb. 20.26	2447577.76	CTIO 1.0-m	CS/2DF	Wells
1989 Feb. 21.25	2447578.75	CTIO 1.0-m	CS/2DF	Wells
1989 Feb. 21.41*	2447578.91	Lick 1.0-m	CS/CCD	Filippenko/Richmond
1989 Feb. 23.22	2447580.72	CTIO 1.0-m	CS/2DF	Fernandez
1989 Feb. 24.21	2447581.71	CTIO 1.0-m	CS/2DF	Phillips
1989 Feb. 25.22	2447582.72	CTIO 1.0-m	CS/2DF	Heathcote
1989 Feb. 26.25	2447583.75	CTIO 1.0-m	CS/2DF	Heathcote
1989 Feb. 26.38*	2447583.88	Lick 1.0-m	CS/CCD	Richmond
1989 Feb. 27.25	2447584.75	CTIO 1.0-m	CS/2DF	Heathcote
1989 Feb. 28.21	2447585.71	CTIO 1.0-m	CS/2DF	Wells
1989 Mar. 1.21	2447586.71	CTIO 1.0-m	CS/2DF	Wells
1989 Mar. 1.41	2447586.91	Whipple 1.5-m	Z-machine	Whipple Obs. Staff
1989 Mar. 2.21*	2447587.71	CTIO 1.0-m	CS/2DF	Wells
1989 Mar. 2.33	2447587.83	Whipple 1.5-m	Z-machine	Whipple Obs. Staff
1989 Mar. 3.24	2447588.74	CTIO 1.0-m	CS/2DF	Wells
1989 Mar. 4.26	2447589.76	CTIO 1.0-m	CS/2DF	Wells
1989 Mar. 8.31	2447593.81	Whipple 1.5-m	Z-machine	Whipple Obs. Staff
1989 Mar. 10.23	2447595.73	CTIO 1.0-m	CS/2DF	Phillips
1989 Mar. 13.28	2447598.83	Whipple 1.5-m	Z-machine	Whipple Obs. Staff
1989 Mar. 16.19*	2447601.69	CTIO 1.0-m	CS/2DF	Phillips
1989 Mar. 28.12	2447613.62	CTIO 1.0-m	CS/2DF	Lutz
1989 Mar. 29.47*	2447614.97	Lick 3.0-m	CS/CCD	Filippenko/Shields
1989 Mar. 30.36	2447615.86	MMT	Red Channel	Kirshner
1989 Apr. 5.43	2447621.93	Whipple 1.5-m	Z-machine	Whipple Obs. Staff
1989 Apr. 11.23	2447627.73	Whipple 1.5-m	Z-machine	Whipple Obs. Staff
1989 Apr. 15.09	2447631.59	CTIO 4.0-m	CS/CCD	Ruiz
1989 Apr. 15.24*	2447631.74	Lick 1.0-m	CS/CCD	Richmond
1989 Apr. 19.97*	2447635.47	CTIO 4.0-m	CS/CCD	Heathcote
1989 Apr. 20.08*	2447636.58	CTIO 4.0-m	CS/CCD	Heathcote
1989 Apr. 27.41	2447643.91	Lick 3.0-m	CS/CCD	Filippenko/Shields
1989 Apr. 28.41	2447644.91	Lick 3.0-m	CS/CCD	Filippenko/Shields
1989 May 2.??	2447648.??	CTIO 4.0-m	CS/2DF	Heathcote
1989 May 2.14	2447648.64	Whipple 1.5-m	Z-machine	Whipple Obs. Staff
1989 May 9.07	2447655.57	CTIO 1.5-m	CS/CCD	Phillips
1989 May 10.42*	2447656.92	MMT	Red Channel	Kirshner
1989 May 30.06	2447676.56	CTIO 1.0-m	CS/2DF	Wells
1989 Jun. 3.18	2447680.68	Whipple 1.5-m	Z-machine	Whipple Obs. Staff
1989 Jun. 15.04	2447692.54	CTIO 1.5-m	CS/CCD	Hamuy
1989 Jul. 10.23*	2447717.73	Lick 3.0-m	CS/CCD	Filippenko/Shields
1990 Jan. 4.29*	2447895.79	CTIO 4.0-m	CS/CCD	Phillips
1990 Jan. 20.47	2447911.97	Lick 3.0-m	CS/CCD	Filippenko/Shields

*Plotted in Figure 6. The 2 spectra taken on Jan. 31 1989 and the three taken in mid-April have been combined into single spectra.

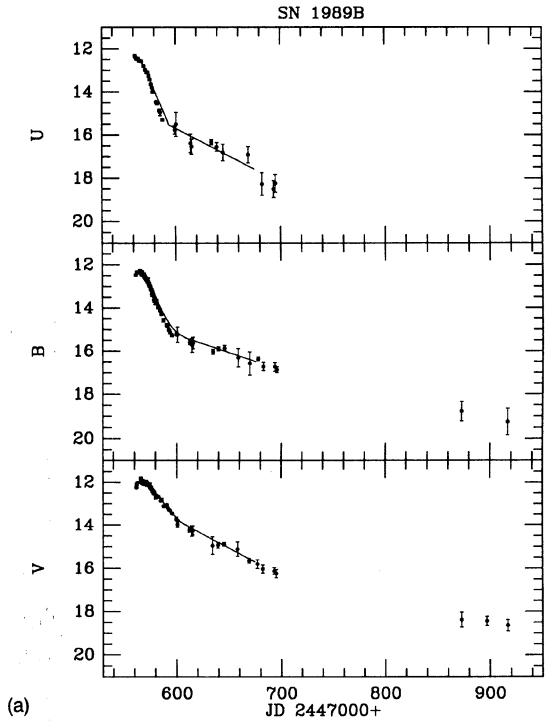

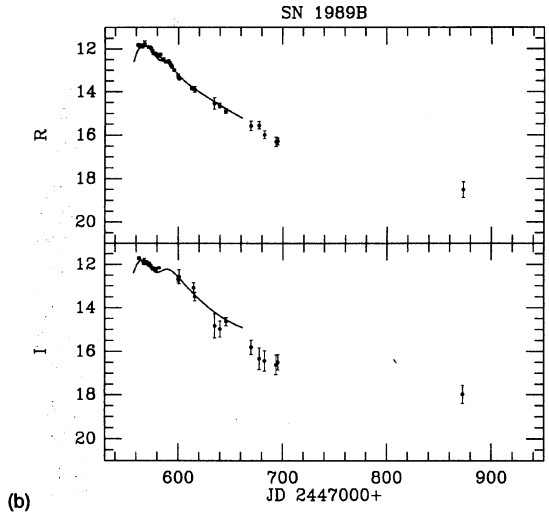

FIG. 2. (a) *U*, *B*, and *V* light curves of SN 1989B. Plotted as solid lines are the Type Ia template curves given by Leibundgut (1988). (b) *R* and *I* light curves of SN 1989B. Plotted as solid lines are the smoothed composite light curves of SN 1991M, SN 1991T, and SN 1992G (Ford *et al.* 1993), which have been shifted to fit the data.

figure are smoothed versions of the composite *R* and *I* light curves of the type Ia events 1991M, 1991T, and 1992G plotted in Fig. 6 of Ford *et al.* (1993). These composite curves

TABLE 8. SN 1989B light curve properties.

Filter	t_o (J.D.)	m_{max} (mags)	$m(t_o^B)$ (mags)	β(7-30) (mags/100 days)	γ(42-131) (mags/100 days)
B	2447565.3(1.0)	12.34(.05)	12.34(.05)	11.4(.1)	1.4(.1)
V	2447567.6(1.0)	11.99(.05)	12.02(.05)	5.8(.1)	2.4(.2)
U			12.51(.05)	15.3(.3)	2.5(.4)

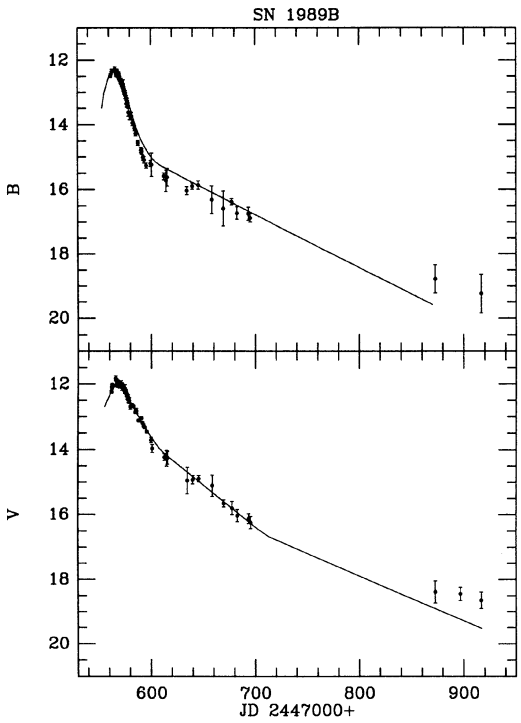

FIG. 3. *B* and *V* light curves of SN 1989B. Shown for comparison are the template curves published by Doggett & Branch (1985).

were defined by Ford *et al.* with respect to the epoch of *V* maximum; hence, the horizontal adjustment of the composite light curves to the observations of SN 1989B was accomplished by assuming $t_0^V - t_0^B = 2$ days. The vertical adjustment was then performed by matching the composite curves to the observed *R* and *I* magnitudes of SN 1989B at t_0^B. As may be seen, although some small differences exist, the composite curves provide a fairly good fit to the SN 1989B observations. Note in particular that, in spite of the 17-day gap in our coverage of the *I* light curve of SN 1989B between JD 2447582–2447599, the inflections or "dips" noted by Ford *et al.* in the composite *R* and *I* light curves ~12 days after *B* maximum are also clearly present in our observations of SN 1989B. These features are almost certainly related to the dips observed in the *JHK* light curves of SNe Ia at approximately the same epoch (Elias *et al.* 1981, 1985). The origin of the broadband dips has recently been attributed not to absorption but to the lack of emission features in these spectral regions (Spyromilio *et al.* 1994).

Returning to the *UBV* light curves displayed in Fig. 2(a), the generally good fits of the Leibundgut templates to the observations indicate that SN 1989B was a typical Ia event. We note, however, that the *U* and *B* light curves exhibited a slightly steeper initial decline rate than the template. Also, the bend which occurred approximately 32 days after maximum in the *B* filter is much sharper than predicted by the template. As shown in Fig. 3, this sharp transition in the *B* photometry is also apparent if comparison is made instead with the template curves of Doggett & Branch (1985). Figure 3 shows that during the year following maximum, SN 1989B

TABLE 9. Comparison of the β and Δm_{15} parameter.

	β (mags/100 days)		Δm_{15} (mags)	
SN	B	V	B	V
1980N	10.5(.3)	6.5(.2)	1.28(.05)	0.73(.05)
1981B	10.4(.4)	5.7(.3)	1.10(.07)	0.55(.08)
1986G	12.6(.7)	8.2(.1)	1.73(.07)	1.10(.07)
1989B	11.4(.1)	5.8(.1)	1.31(.07)	0.71(.07)
1990N	11.2(.5)	5.9(.3)	1.01(.10)	0.66(.10)
1991T	9.9(.4)	5.2(.2)	0.94(.07)	0.53(.06)
1991bg	15.5(.6)*	11.9(.5)*	1.88(.10)	1.37(.03)

*Decline rate measured between days 4-14 after t_o^B

declined in brightness somewhat less steeply than other SNe Ia. However, we are not sufficiently confident in the background corrections applied to the photometry obtained at the latest epochs to consider this disagreement significant.

In columns (4) and (5) of Table 8, we list for the *UBV* light curve of SN 1989B the observed rate of dimming (β) during the fast-decline phase between days 7 and 30 after t_0^B, and the rate of the slow-decline phase (γ) as calculated in the interval 42–131 days.[17]

The values of β for the B and V light curves are compared in Table 9 with measurements carried out in an identical fashion for the well observed SNe Ia 1980N (Hamuy *et al.* 1991), 1981B (Branch *et al.* 1983), 1986G (Phillips *et al.* 1987), 1990N (Leibundgut *et al.* 1991), 1991T (Phillips *et al.* 1992), and 1991bg (Filippenko *et al.* 1992b; Leibundgut *et al.* 1993). However, as discussed briefly by Hamuy *et al.* (1991), the β parameter is difficult to measure in a consistent fashion due to both observational errors and incomplete coverage of the light curves. After some experimenting, Phillips (1993) found that a parameter which is more precisely measured and which provides better discrimination is the total magnitude which the light curve declines from maximum to 15 days past maximum. Measurements of this parameter, which he called Δm_{15}, for the same six SNe Ia are included in Table 9. These data provide clear evidence for a significant dispersion in the initial decline rates of SNe Ia, with the light curves of SN 1989B being fairly representative of the mean.

Extensive optical photometry of SN 1989B has been published by BBCRT, TKVBI, and Volkov (1991). A comparison of the B and V data with our observations is shown in Fig. 4. As may be seen, even at maximum there are significant differences between our measurements and these three sets of photometry. The magnitudes given by TKVBI are generally brighter than our results, with the discrepancy at maximum amounting to nearly a half magnitude. The same applies to the U photometry presented by these authors (which is not illustrated). The photometry of BBCRT tends to fall below ours. These differences are not likely to be due to the local standards employed, since the photometry for the stars measured in common agrees to within a few percent. Nor is it probable, in either case, that the discrepancies are the result

[17]The β and γ parameters are originally due to Pskovskii (1967, 1977, 1984), but the definitions employed here are those given by Hamuy *et al.* (1991).

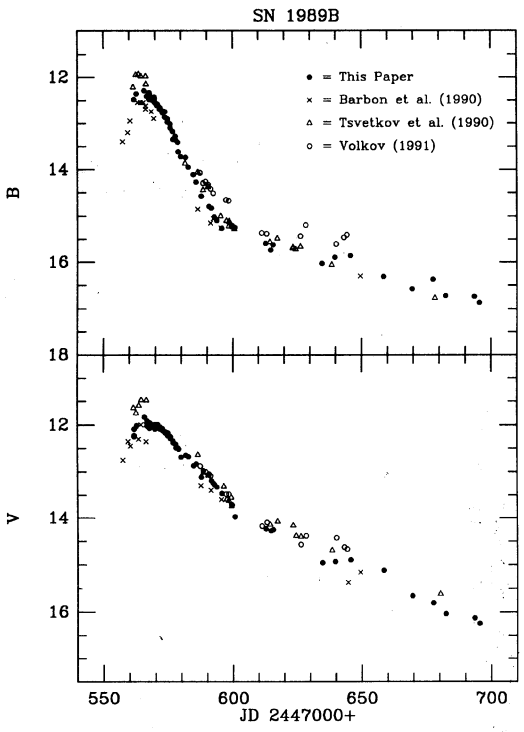

FIG. 4. Comparison of the B and V photometry of SN 1989B given in this paper with the published results of Barbon *et al.* (1990), Tsvetkov *et al.* (1990), and Volkov (1991).

of errors in the corrections applied for the background light of NGC 3627 since this would affect the photometry carried out at later epochs much more than that obtained at maximum. A substantial fraction of the photometry of both BBCRT and TKVBI was carried out with photographic plates, and such measurements are susceptible to error in the presence of a strong and nonuniform background. The late time photometry of Volkov (1991) has most certainly not accounted for the background galaxy light. We are confident of the accuracy of our own results since the majority of the measurements were obtained with CCD detectors, and the background corrections were obtained from images acquired when the supernova had completely faded from detection.

3.2 Color Curves

Figures 5(a) and 5(b) show the $U-B$, $B-V$, $V-I$, and $R-I$ colors of SN 1989B plotted as a function of time since B maximum. Overplotted in Fig. 5(a) are Leibundgut's (1988) template curves for $U-B$ and $B-V$. The spike in the $U-B$ template is an artifact of the construction of the curve and should not be taken as a real feature. For the zero points of the templates, we have assumed that the colors at B maximum of a typical unreddened SN Ia are $(U-B)_0=-0.19$ mags and $(B-V)_0=+0.01$ mags, as measured by Hamuy *et al.* (1991) for SN 1980N in NGC 1316 (see also Capaccioli *et al.* 1990). Figure 5(a) shows that both the $U-B$ and $B-V$ data are offset from the templates by several tenths of a magnitude, which almost certainly is due to interstellar

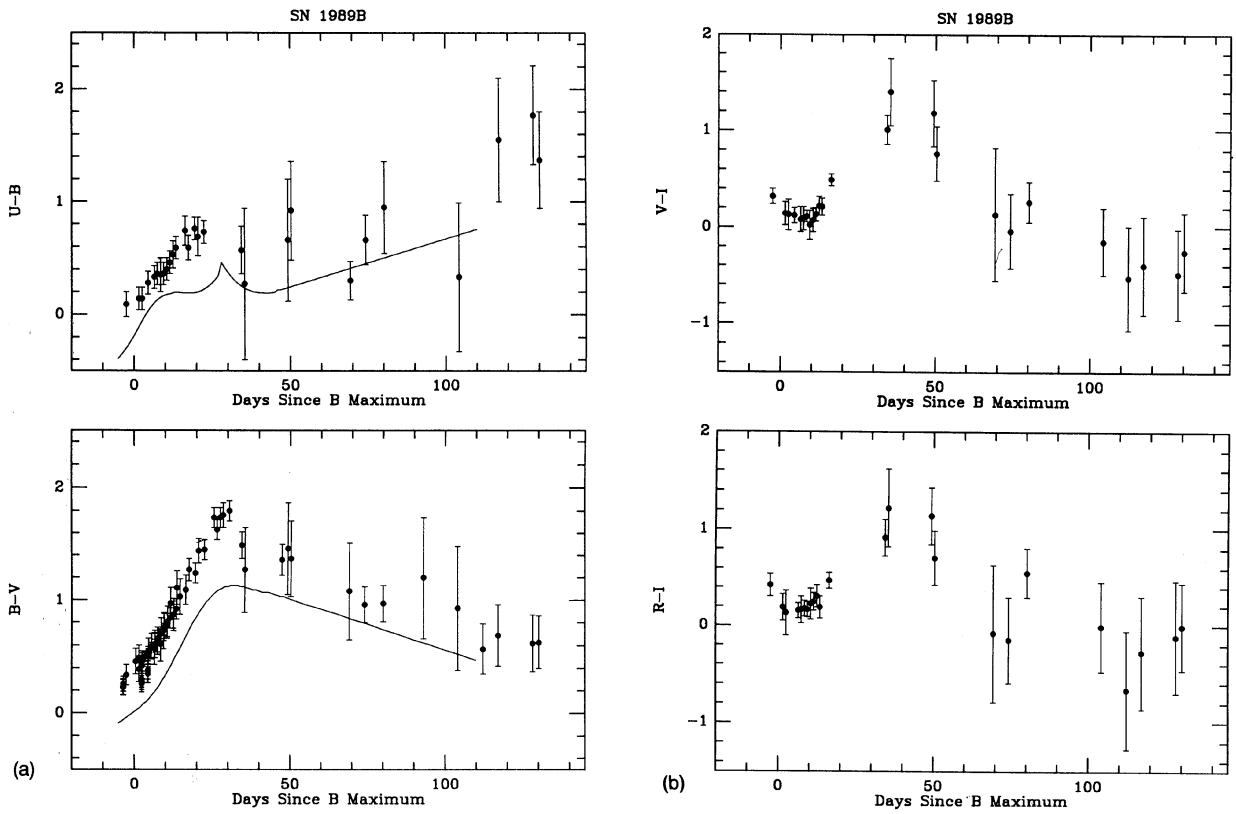

FIG. 5. (a) Observed $U-B$ and $B-V$ color evolution of SN 1989B. Plotted as solid lines are the template curves of Leibundgut (1988). (b) Observed $V-I$ and $R-I$ color evolution of SN 1989B.

reddening within NGC 3627 (see Sec. *3.4*). Otherwise, the $B-V$ observations match the shape of the template reasonably well, although the inflection in color which takes place 30 days after B maximum is much sharper in the data than in the template. A similar effect was observed by Hamuy *et al.* (1991) for SN 1980N. The shape of the $U-B$ color evolution is quite different from the template, particularly over the first 20–30 days. The $V-I$ and $R-I$ color evolutions superficially resemble that observed in $B-V$, but cover a significantly smaller range in color.

3.3 Optical Spectral Evolution

Owing to the superb summer observing conditions that routinely occur in the north of Chile, we were able to obtain low-dispersion optical spectra of SN 1989B on essentially a nightly basis at CTIO for the first month following discovery. Combining these observations with spectra obtained at Lick, Mt. Hopkins, the MMT, and KPNO provides an unprecedented look at the early evolution of a Type Ia supernova. A sampling of these spectral data covering the period from six days before B maximum to nearly a year after is shown in Fig. 6. The blueshifted Si II λ6355 absorption feature observed strongly in the spectrum the first two weeks after discovery combined with the absence of hydrogen lines at all phases clearly identifies this supernova as a Type Ia event. Comparison of the spectra in Fig. 6 with observations of the prototypical SNe Ia 1937C (Minkowski 1939), 1972E (Kirshner *et al.* 1973), and 1981B (Branch *et al.* 1983) shows that the spectral evolution of SN 1989B was typical in nearly all respects—the only real exception being the redder color of the continuum observed at all phases [consistent with the $U-B$ and $B-V$ color offsets observed in Fig. 5(a)]. The maximum-light spectrum, which was characterized by broad absorption features due to Ca II, Mg II, Si II, S II, and O I, slowly gave way to one dominated by lines of Fe-group elements during the first two weeks following B maximum. Clearly visible in all of the spectra is narrow Hα emission due to an underlying H II region in a spiral arm of NGC 3627 [see Fig. 1 for indicated position]. Measurements of the large number of spectra obtained on the CTIO 1.0 m telescope yield a mean heliocentric velocity for this emission of 638 ± 30 km s^{-1} which agrees quite well with the value reported by BBCRT. Also present in the spectra are strong narrow lines of Na I D and Ca II H & K which presumably originate from interstellar gas in the disk of NGC 3627. From our three highest-dispersion spectra, we measure a mean heliocentric velocity of 546 ± 33 km s^{-1} for the Ca II H & K lines, which is in good agreement with the value of 536 ± 9 km s^{-1} reported by Bolte *et al.* (1989) for the Na I D lines and in fair agreement with the measurement by BBCRT of 580 ± 20 km s^{-1} (also for the Na I D lines).

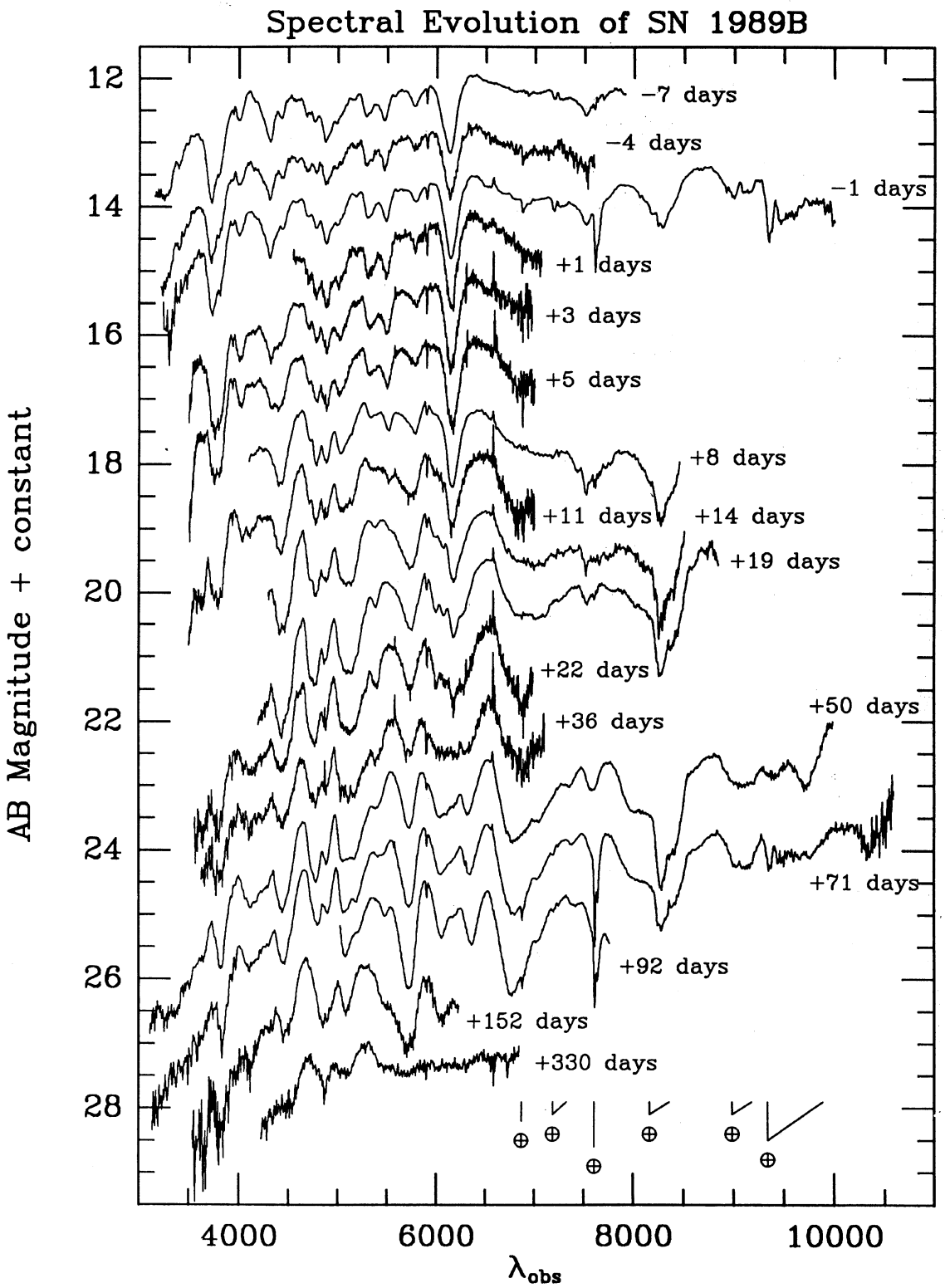

FIG. 6. A sampling of optical spectra obtained of SN 1989B illustrating the evolution from six days before *B* maximum to nearly a year after. The spectra are plotted on an *AB* magnitude scale ($AB = -2.5 \log F_\nu - 48.595$), but are shifted vertically with respect to each other by arbitrary amounts. Note that absorption features of terrestrial origin (indicated by the symbol ⊕ at the bottom of the figure) have not been removed from the spectra for −1, +71, and +92 days. The spectrum corresponding to −7 days is the sum of the two spectra obtained on 1989 Jan 31, and that labeled +71 days is the combination of the three spectra obtained on 1989 Apr 15, 19, and 20 (see Table 7).

TABLE 10. Absorption line radial velocities.

Julian Date	Ca II H & K	Mg II λ4481 (km/sec)	Si II λ6355
2447557.70	-17081	-12178	
2447557.80	-16571	-11886	-11683
2447557.97	-15687	-11755	-11069
2447558.94	-15194	-12044	-11552
2447561.05			-10817
2447561.80		-11669	
2447561.92	-14197	-11510	-10451
2447562.05	-15106	-11704	-10493
2447562.82		-11533	
2447563.85	-14518	-11776	-10544
2447564.89	-13557	-11434	-10484
2447565.82			-10477
2447567.81	-13679	-11014	-10418
2447569.78	-12758	-10751	-9929
2447571.79	-12234		-9938
2447571.91			-9956
2447572.95			-9613
2447573.80	-12002		-9845
2447575.79	-11883		-9746
2447576.77	-11627		-9585
2447577.76	-12029		-9399
2447578.75			-9381
2447578.91			-8957
2447580.72	-12023		-9208
2447581.71	-11873		-9434
2447582.72	-11915		-9303
2447583.75	-11838		-8870
2447583.88			-8833
2447584.75	-11451		-8910
2447585.71	-11881		-9253
2447586.71	-11545		-9166
2447586.91	-11761		-9053
2447587.71	-11237		-9057
2447587.83			-8807
2447588.74	-11740		-8793
2447589.76	-11863		-8623
2447593.81			-8669
2447595.73	-10879		-8661
2447598.78			-8390
2447601.69	-11058		
2447614.97	-9426		
2447621.93	-9305		
2447631.59	-8774		
2447636.58	-8651		
2447643.91	-8477		
2447655.57	-8760		
2447717.73	-9505		

Measurements of the radial velocity of the minimum of the Si II λ6355 absorption made from our spectra are listed in Table 10. These have been corrected to the rest system of the supernova using a velocity of 638 km s^{-1}, consistent with the value yielded by the underlying H II region emission. Similar measurements of the Mg II λ4481 absorption[18] at early epochs (before this feature became blended with other features) and the Ca II H & K absorption are also given in

[18]Although we refer to this feature as Mg II λ4481, lines of Fe II and Fe III also contribute to the observed absorption. In SN 1991T, the feature started out as Fe III and probably evolved to Fe II without ever being primarily Mg II (Jeffery *et al.* 1992).

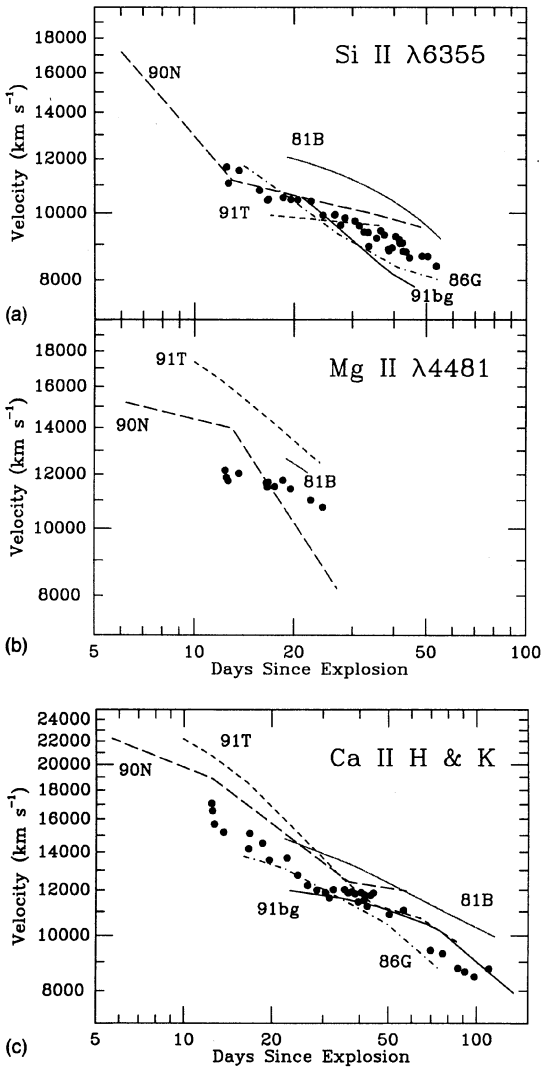

FIG. 7. (a) Expansion velocities inferred from the absorption minimum of the Si II λ6355 line vs. time since explosion. A time difference of 20 days is assumed between explosion and *B* maximum. The measurements for SN 1989B are plotted and compared with similar velocity data for the SNe Ia 1981B, 1986G, 1990N, 1991T, and 1991bg. (b) Same as in Fig. 7(a), but for the Mg II λ4481 absorption minimum. (c) Same as in (a), but for the Ca II H & K absorption minimum.

Table 10. A comparison of these velocities with analogous data for SN 1981B (Branch *et al.* 1983), SN 1986G (Phillips *et al.* 1987), SN 1990N (Leibundgut *et al.* 1991), SN 1991T (Phillips *et al.* 1992), and SN 1991bg (Leibundgut *et al.* 1993) is shown in Fig. 7. Note that the data in these diagrams are plotted as a function of time since explosion, assuming an interval of 20 days between explosion and *B* maximum (see Leibundgut *et al.* 1991). The evolution of the Si II velocities in SN 1989B was fairly similar to that observed for SN 1986G and SN 1990N, but offset to lower velocities with respect to the measurement of SN 1981B. The Si II 6355 data confirm the findings of Branch (1987) and Branch *et al.* (1988) of significant differences in the velocity evolution of this line among SNe Ia of otherwise similar spectral charac-

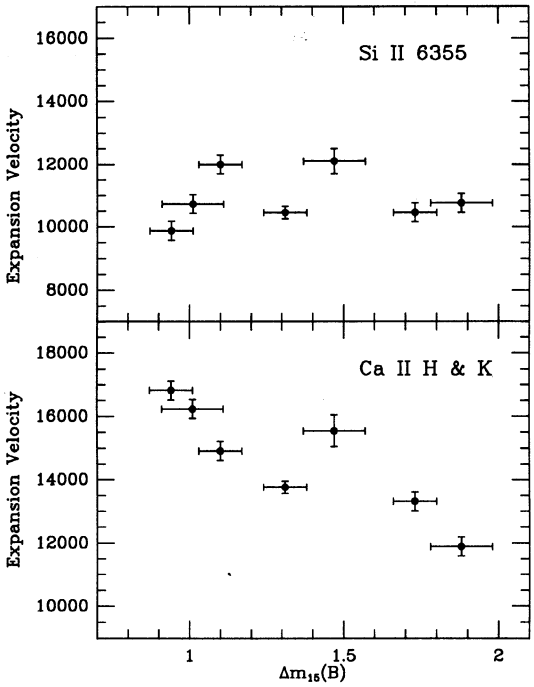

FIG. 8. (a) The decline rate parameter $\Delta m_{15}(B)$ is plotted vs the expansion velocity for the Si II λ6355 measured at B maximum for seven SNe from Phillips (1993) sample. (b) The same is plotted for the Ca II H & K lines for the same sample.

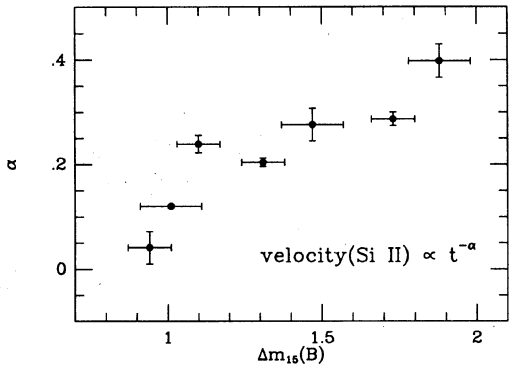

FIG. 9. The decline rate parameter $\Delta m_{15}(B)$ is plotted vs the power law index for temporal decrease in the Si II λ6355 velocity for the seven SNe from the Phillips (1993) sample.

teristics. Within the observed dispersion, however, the velocity evolution of all three features seems to have been fairly typical. The radial velocity measurements of the Mg II λ4481 plotted in Fig. 7 reveal similar differences between SN 1981B, SN 1986G, SN 1989B, and SN 1990N.

Following Pskovskii (1977, 1984) and Branch (1981), evidence for possible correlations between expansion velocity and decline rate was examined. These authors found that the velocity of the Si II λ6355 absorption near maximum light was correlated with the value of Pskovskii's β parameter. However, as illustrated in Fig. 8, no such relationship is apparent in the SNe Ia in the Phillips (1992) sample. (Although the Si II velocity is plotted versus $\Delta m_{15}(B)$ in Fig. 8, no correlation is observed versus Pskovskii's β parameter either.) On the other hand, Fig. 8 shows that the velocity of the Ca II H & K minimum may be much more closely correlated with $\Delta m_{15}(B)$. It is unclear why one line should be correlated with decline rate while the other is not.

Curiously, while the expansion velocity derived from the Si II λ6355 line at maximum does not appear to correlate with decline rate, there is a suggestion in the data that the rate of decrease of the expansion velocity in this line during the first weeks following maximum light does depend on the decline rate. In the case of the slowest-declining SNe (1991T and 1990N), the expansion velocity of the Si II line changes only very slowly during the first month following maximum. Conversely, for the SNe with steep light curves (1991bg and 1986G), the Si II velocity displays the fastest decrease with time. Figure 9 illustrates this correlation, where the B light curve decline rate parameter $\Delta m_{15}(B)$ is plotted versus the power law index, α, obtained from fits of the Si II λ6355 velocities (measured over the period extending from a week before maximum to approximately a month after) to the equation $v \propto t^{-\alpha}$, where v is the velocity. As discussed by Branch *et al.* (1988), if the variation of density with velocity in the ejected matter is represented by a power law, $\rho \propto v^{-n} t^{-3}$, and the opacity is assumed to be constant, the photospheric velocity will vary as $t^{-2/(n-1)}$. The range of values of the power law index α observed in Fig. 9 corresponds to $n = 6-51$. The apparent existence of a correlation between α and $\Delta m_{15}(B)$ suggests that the decline rate of the light curve is closely related to the density gradient of the ejecta, with the slowest decline rates occurring in those SNe having the steepest density gradients in their outer envelopes. However, the assumption of constant opacity, which is true only if the opacity is due purely to electron scattering, is almost certainly incorrect (see Höflich *et al.* 1991, and references therein). Hence, without detailed models, we cannot exclude the possibility that the observed range of values of the power law index α is due instead to differences in the radial variation of the opacity. Some evidence for the latter is found in Fig. 7(b), which suggests that the effect may be the opposite for the Ca II H & K lines—i.e., the largest values of α are observed for the slowest declining events (SNe 1991T and 1990N). Alternatively, the very small change with time of the Si II velocity in an event like SN 1991T may simply mean that the Si is confined to a narrow velocity interval in the expanding ejecta.[19]

[19]Part of the observed spread in α may also be due to the assumption that all SNe Ia take 20 days to rise to B maximum. Indeed, the evidence to date suggests that the faster-declining events also have the shortest rise times from explosion to maximum (Suntzeff 1994). However, even if we assume that the fastest-declining SN in our sample, 1991bg, rose to maximum in only 10 days, the value of α measured from the Si II λ6355 line for this object would change from 0.40 ± 0.03 to 0.26 ± 0.01, which is still significantly greater than the value of 0.04 ± 0.03 measured for the slowest-declining event, SN 1991T, for an assumed rise time of 20 days.)

3.4 Interstellar Extinction

The red color of SN 1989B at B maximum ($B-V=0.32$ mags), the offsets observed between the $U-B$ and $B-V$ color evolutions and the Leibundgut templates, and the strong interstellar Ca II and Na I D absorption lines present in the optical spectra are all consistent with the presence of significant interstellar reddening. One of the standard methods of estimating the interstellar reddening of SNe Ia is to compare the observed $B-V$ color at B maximum with an assumed intrinsic (i.e., reddening-free) color at this phase. A variation on this technique is to calculate the shift of the observed $B-V$ color evolution with respect to an assumed template of the reddening-free color evolution of SNe Ia. This is the method employed by BBCRT who derived a reddening for SN 1989B of $E(B-V)=0.81$ mags. This result is much greater than the value of 0.32 which we derive by shifting the Leibundgut (1988) template with respect to our own photometry [see Fig. 5(a)], but this is due to different assumptions of the zero point of the template $B-V$ curve rather than to differences between the observations. In particular, the template used by BBCRT assumes an intrinsic color at B maximum of $(B-V)_0=-0.35$ mags, which is very much bluer than the value of 0.01 that we have adopted based on the work of Capaccioli *et al.* (1990) and Hamuy *et al.* (1991).

Rather than just using B and V, a potentially more powerful way to estimate the reddening of SN 1989B is to compare the photometry obtained in all eight colors (*UBVRIJHK*) with comparable observations of an unreddened SN Ia. We have performed such a calculation with respect to the well observed SN 1980N (Hamuy *et al.* 1991; Elias *et al.* 1981, 1985) which occurred in the outskirts of the peculiar early-type galaxy NGC 1316. As Phillips (1993) has noted, the decline rate parameter $\Delta m_{15}(B)$ for these two SNe I are essentially identical (1.28 ± 0.05 versus 1.31 ± 0.07). Figure 10(a) shows a detailed comparison of the *UBVRI* photometry of these two SNe Ia. On the left-hand side, the data in each color are plotted as a function of time from B maximum without applying any shifts in magnitude. On the right-hand side, the data are plotted with the observations of SN 1980N shifted in magnitude to coincide as best as possible with those of SN 1989B. The magnitude of the shift $[\Delta m_\lambda = m_\lambda(1989B) - m_\lambda(1980N)]$ deduced for each color, which was calculated using a χ^2-minimizing procedure, is indicated in the same figure. Figure 10(b) shows a similar comparison of the *JHK* light curves. If we assume that both supernovae were intrinsically identical events, then the light curve shift, Δm_λ, at any particular wavelength is related to the relative distance modulus, $\Delta\mu$, and relative extinction, ΔA_λ, through the equation

$$\Delta m_\lambda = \Delta\mu + \Delta A_\lambda .$$

Adopting the average interstellar extinction curve given in Table 2 of the review by Savage & Mathis (1979) which tabulates the values of $A_\lambda/E(B-V)$ from 0.1–3.4 μm for an assumed value of $R=A_V/E(B-V)=3.1$, this equation can be rewritten as

$$\Delta m_\lambda = \Delta\mu + \Delta E(B-V) * \left(\frac{A_\lambda}{E(B-V)}\right),$$

where $\Delta E(B-V)$ is the differential color excess between the two supernovae. Figure 11 shows a plot of the shifts, Δm_λ, versus the Savage and Mathis values of $A_\lambda/E(B-V)$. A linear least-squares fit to these data yields a relative distance modulus $\Delta\mu=-1.62\pm0.11$ mags (i.e., SN 1989B lies closer than SN 1980N), and a relative reddening excess of $\Delta E(B-V)=0.37\pm0.03$ mags. The foreground extinction due to our own Galaxy in the line of sight to SN 1989B is most likely negligible (Burstein & Heiles 1982), and Hamuy *et al.* (1991) have argued that SN 1980N was also essentially unreddened. Hence, nearly all of this extinction must be produced by dust in NGC 3627. Note that the excellent fit in Fig. 11 provides strong evidence that the properties of the dust responsible for the reddening of SN 1989B are very similar to those of normal interstellar dust in the disk of our own Galaxy.

A completely independent estimate of the color excess of SN 1989B has been published by Bolte *et al.* (1989), who reported the detection of the λ6284 diffuse interstellar band in high signal-to-noise ratio spectra. Using Herbig's (1975) relationship between the equivalent width of the λ6284 feature and $E(B-V)$, Bolte *et al.* derived $E(B-V)\approx0.8$ mags for SN 1989B. Although Bolte *et al.* do not attach an error to this estimate, a close look at the data used by Herbig shows that the uncertainty must be at least ±0.3 mag, and perhaps even larger if the measurement error of the λ6284 equivalent width for SN 1989B is taken into account. Still, we are surprised at the level of disagreement between this estimate and our own. If the color excess of SN 1989B really is 0.8 mags, then one or more of our assumptions must be incorrect. The evidence that SN 1980N was essentially unreddened is quite strong—hence, we would need to question the assumption that SNe 1980N and 1989B were intrinsically identical events. In this case, however, the excellent fit shown in Fig. 9 becomes difficult to understand. Hence, we conclude that the photometric data do not support the high level of extinction inferred by Bolte *et al.*, but we are unable to pinpoint the likely source(s) of the discrepancy.

4. DISCUSSION

The observations presented in this paper clearly indicate that SN 1989B was a typical Type Ia event in essentially every way. We have shown that the *UBV* light curves agreed quite well with template curves determined from other events of this type. We have also claimed that the optical spectral evolution was typical of other SNe Ia. This is illustrated in further detail in Fig. 12, where we have compared our observations of SN 1989B at B maximum and approximately 50 days later with comparable epoch spectra of two other well observed SNe Ia: SN 1981B (Branch *et al.* 1983) and SN 1986G (Phillips *et al.* 1987). In order to make this

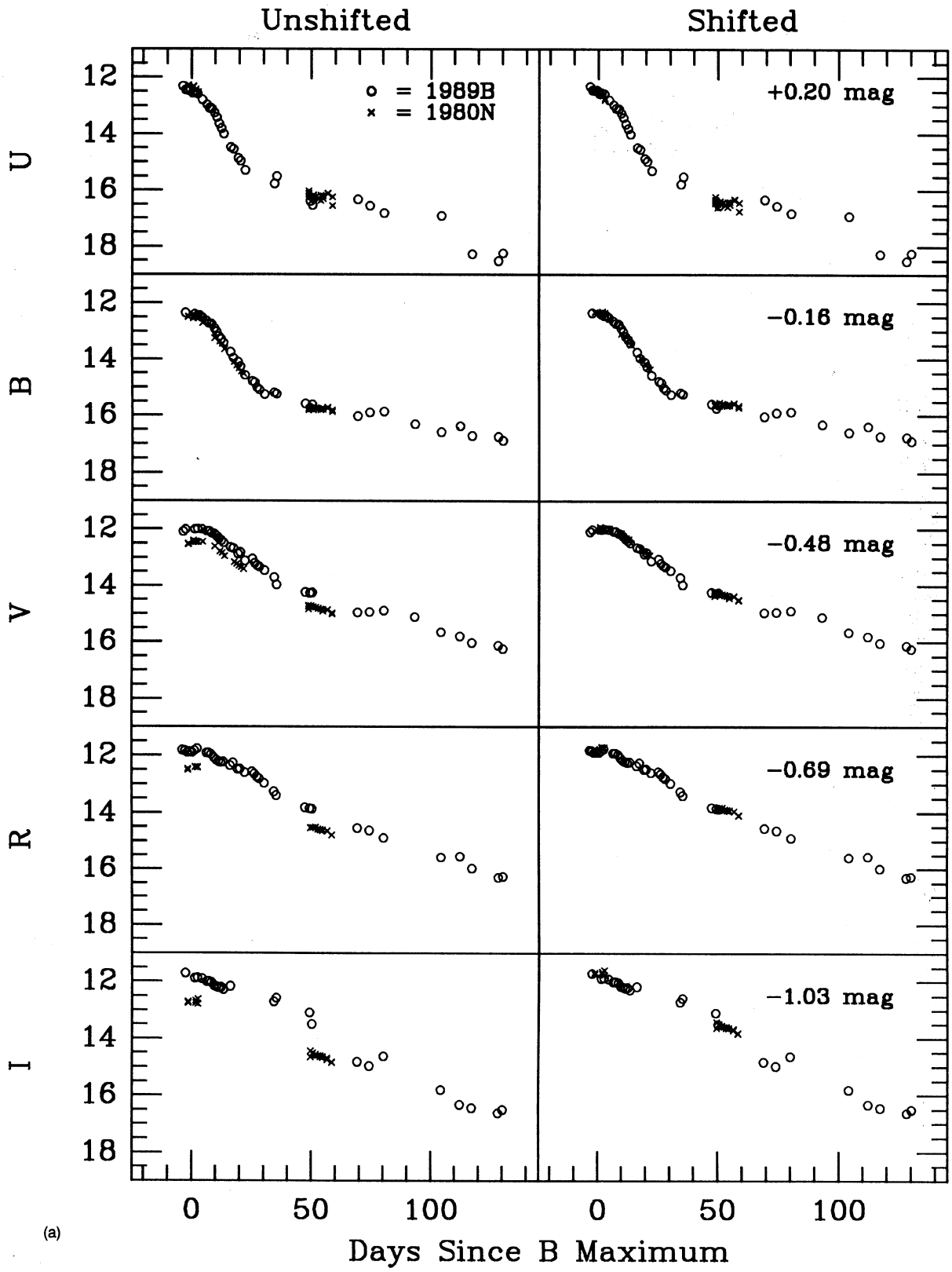

FIG. 10. (a) Comparison of the *U, B, V, R,* and *I* photometry of SN 1989B with photoelectric observations of SN 1980N. The data have been aligned along the time axis using the respective times of *B* maximum, t_0^B. On the left-hand side, the data in each color are plotted without applying any vertical shifts. On the right-hand side, the data are plotted with the photometry of SN 1980N shifted in magnitude to coincide as closely as possible with the light curves of SN 1989B. The resulting magnitude shifts are indicated for each color.

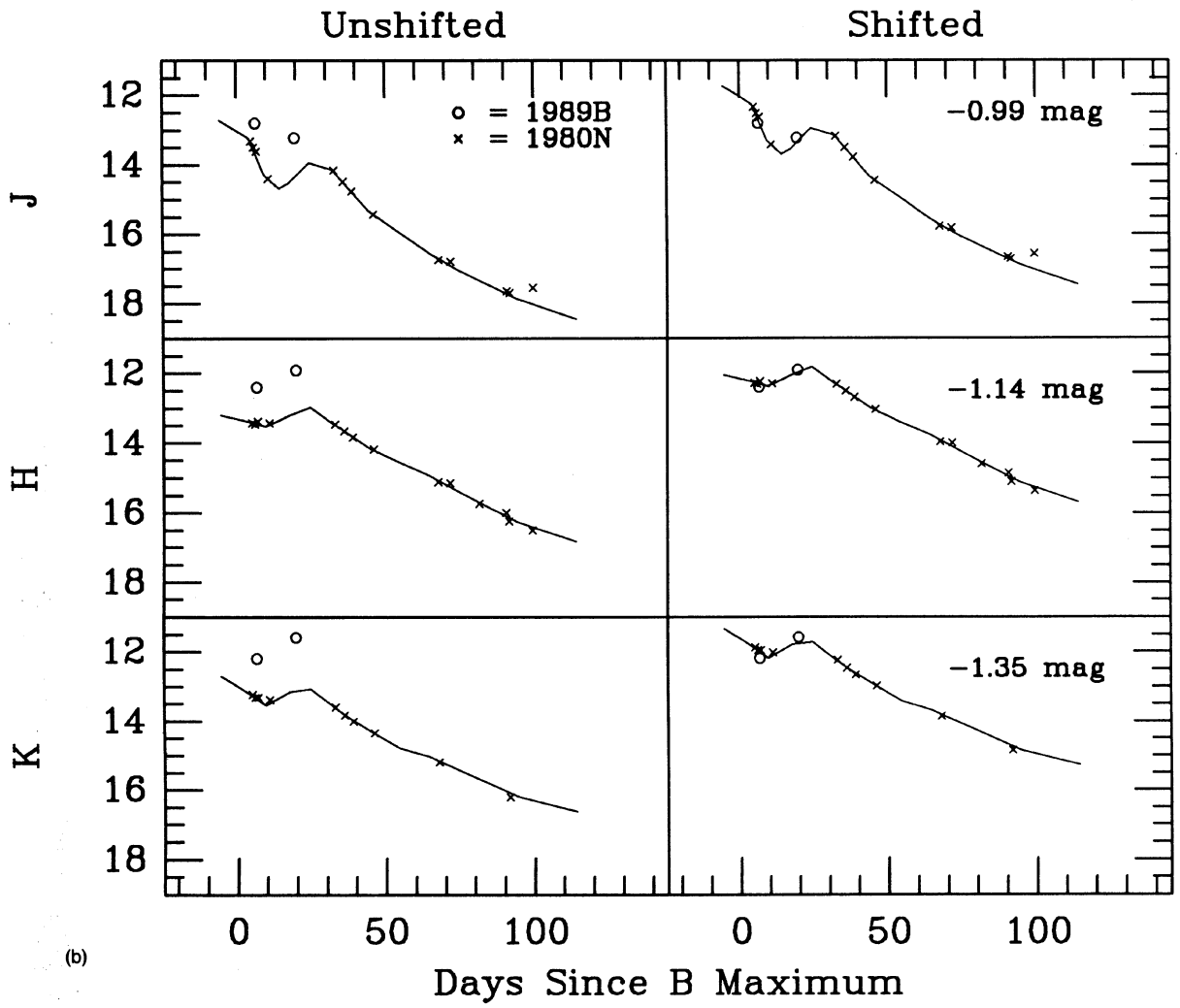

FIG. 10. (b) Similar comparison of the *J*, *H*, and *K* photometry of SNe 1989B and 1980N. Note that the template light curves of Elias *et al.* (1985) are plotted along with the observation of SN 1980N.

plot, we corrected the spectra of SN 1989B for a reddening of $E(B-V)=0.37$ mags (see Sec. *3.4*) and those of SN 1986G by an amount $E(B-V)=0.6$ mags (see Phillips 1993). The resemblance at both epochs is remarkable. Nevertheless, minor differences at maximum light are clearly present—most noticeably in the relative strengths of the S II and Si II lines, the resolution of the blend of Fe II, Si II, and S II absorption lines centered at 4900 Å, and the presence of Ti II absorption near 4150 Å in the spectrum of SN 1986G (Filippenko *et al.* 1992b). The continuum of SN 1986G at maximum is also somewhat redder than the continua of 1981B and 1989B. It should be recalled that significant differences are also observed between these three same supernovae in the velocity evolutions of the Si II λ6355, Ca II H & K, and Mg II λ4481 absorption minima [see Figs. 7(a)–7(c)], and that the *B* and *V* light curves of SN 1986G declined considerably faster than those of either SN 1981B or SN 1989B (see Table 9). Figure 12 clearly shows that the spectral differences are greatest around maximum light when the spectrum is dominated by lines due to intermediate-mass α-nuclei elements, but essentially disappear at later epochs when the spectrum has grown to be dominated by Fe II lines—a point which was recently emphasized by Filippenko *et al.* (1992a) and Phillips *et al.* (1992) for SN 1991T.

In the weeks following *B* maximum, the spectra of SN 1989B evolved in the manner characteristic of SNe Ia. During the first week after maximum, the strong Si II λ6355 absorption remained essentially unchanged. However, blends of P-Cygni lines of Fe II began to dominate other parts of the spectrum. By about 5 days past maximum, Fe II absorption at ~4400 Å had strengthened appreciably and the Mg II λ4481 line had essentially disappeared. By day +8, absorption due to Fe II λ4923, 5018, 5169 (multiplet 42) had grown to dominate the spectral region in the range 4600–5200 Å, and two apparent emission features at ~4800 and ~5000 Å had appeared. By this date, the blue component of the "W-shaped" S II absorption feature at ~5200–5500 Å (see Fig. 6) had nearly vanished. The rapid growth of the absorption at

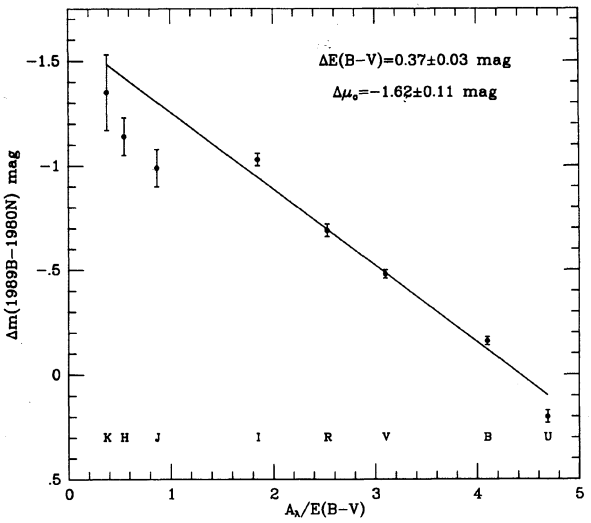

FIG. 11. Plot of the magnitude shifts, Δm_λ, determined from Fig. 8 vs the adopted reddening curve values, $A_\lambda/E(B-V)$. Plotted as a solid line is a least-squares fit to the data.

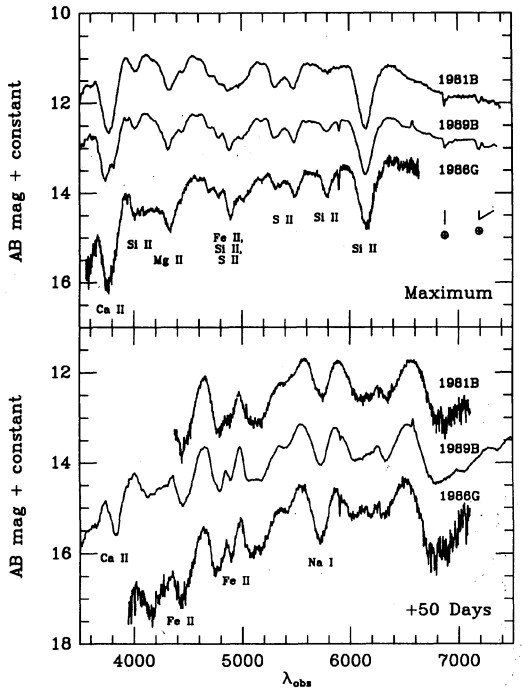

FIG. 12. Comparison of the spectra of SN 1989B at *B* maximum and approximately 50 days later with comparable epoch spectra of the well observed SNe Ia 1981B and 1986G. Note that the spectra of SNe 1989B and 1986G are corrected for assumed reddening values of $E(B-V)=0.37$ and 0.60, respectively. Absorption features of terrestrial origin (indicated by the symbol ⊕) have not been removed from the data except in the case of the SN 1989B spectrum obtained at +50 days.

~5800 Å and the related peak at ~5900 Å is probably associated with the emergence of Na I D rather than a strengthening of Si II λ5972. At later epochs, however, the peak at ~5900 Å has traditionally been associated with a blend of [Co III] emission lines (see below), and its decay is the principal evidence for the radioactive decay mechanism in SN Ia events (Axelrod 1980; Kuchner *et al.* 1994).

By 11 days after maximum, the Fe II absorption feature at ~4400 Å and the associated peak at ~4600 Å had fully developed, leaving no sign of the Mg II λ4481 line. The blue component of the S II feature at 5000–5200 Å had also disappeared and the red component was only weakly present. At this epoch the Si II λ6355 absorption began to noticeably weaken. Three days later, the Si II absorption had grown still weaker and the S II feature had disappeared, while the P-Cygni absorption due to the Na I D lines had grown to obliterate the Si II λ5972 absorption. At this phase a broad emission feature centered at ~6600 Å due to a blend of Fe II lines rapidly increased in strength as the Si II λ6355 absorption faded. Over the next few days the Si II feature continued to weaken, until it finally disappeared around day +25. At this point the spectrum was nearly entirely due to blends of emission lines of Fe-peak elements.

The transition in the character of the spectrum of a typical SN Ia, from being dominated by intermediate mass elements to being dominated by Fe II, has been noted previously (Branch *et al.* 1983), but not in the temporal detail afforded by our observations of SN 1989B. In the theoretical models (Harkness 1991, and references therein), it corresponds to the recession of the photosphere from the outer partially unburned layers into the inner iron-peak matter. This transition is thus of crucial importance to constrain both the dynamical and atmospheric models of SNe Ia. Figure 6 shows that for SN 1989B it occurred ~10–12 days after maximum light, at about the time the light curve begins its approximately linear descent (in *B*) from maximum. The spectrum is nearly completely iron-peak dominated by day +20. This is somewhat before the bend in the light curve at approximately +30 days that signals the onset of the long-term linear ^{56}Co-powered phase of the light curve. The dominance of Fe-peak matter is also approximately coincident with the onset of the temporary minimum in the infrared that is characteristic of SN Ia events (Elias *et al.* 1981, 1985). The current results suggest that the broad band dips may be related to Fe-peak elements in some way.

After this initial transition, Fig. 6 shows that the evolution of the spectrum of SN 1989B from dominance by permitted lines of Fe II to the nebular phase where lines of [Fe II] 4355, 4980, 5340, 7200 Å; [Fe III] 3950, 4690, 4980, 5240 Å; and [Co III] 5880, 6540 Å prevail occurred only very gradually. At day +18, on about 25 February, there are two Fe blends at 5300 and 5400 Å which are of about equal strength. By day +24, the latter has grown to dominate. By about day +80, however, this feature has shrunk to become less strong than the Na I D/[Co III] peak at 5900 Å and is roughly equivalent to the peak at 5300 Å. After this epoch the feature at 5300 Å dominates and by day 100 it is somewhat stronger than the Na/Co feature. Over the same epoch new, somewhat smaller peaks come in at 6100–6300 Å. It seems likely that these changes, which have never before been observed in this detail, actually represent the transition to the "nebular" phase.

The narrow Na I D interstellar absorption lines in SN

1989B serve as a convenient reference point in studying the evolution of the Na I D/[Co III] peak at 5900 Å. From 7 to 20 days after B maximum, this narrow absorption nearly bifurcates the P-Cygni peak associated with Na I D in the supernova. Note, however that the bulk of the flux is to the blue of the narrow absorption component in the spectra obtained 30–50 days after maximum, and the absorption minimum at 5750 Å has shifted slightly to the blue. The flux is once again nearly equally distributed on either side of the narrow absorption by day +100. It is not clear that there is any associated shift of the absorption component. These subtle shifts in this feature may be consistent with the onset of the [Co III] and then its subsequent fading by radioactive decay (see also Kuchner *et al.* 1994). However, it is clearly of great importance to deconvolve the effects of the changes due to the decay of radioactive cobalt from those associated only with the changes of the physical conditions of the Na and Co.

As a by-product of our technique for estimating the reddening of SN 1989B with respect to SN 1980N in NGC 1316, a relative distance modulus $\Delta\mu=-1.62\pm0.11$ mags for these two events was derived (see Sec. *3.4*). It is interesting to compare this number with independent estimates of the distances of NGC 3627 and NGC 1316. In his study of the absolute magnitudes of SNe Ia, Phillips (1993) quotes a Tully–Fisher distance for NGC 3627 due to Pierce (1994) of $\mu_{\rm NGC\ 3627}=29.4\pm0.3$ mags, and a surface brightness fluctuations (SBF) distance to NGC 1316 of $\mu_{\rm NGC\ 1316}=31.02\pm0.12$ mags (Tonry 1994), implying a relative distance modulus of $\Delta\mu=-1.62\pm0.25$ mags which agrees with our estimate based on the two supernovae. Once again, this provides strong evidence that the properties of the dust which reddened SN 1989B were similar to those of the dust in the disk of our own Galaxy. Moreover, the ratio of total to selective absorption, $R[=A_V/E(B-V)]$, must have been very close to the value of ~3 which is observed for dust in our own Galaxy, in contradiction to the conclusion reached by Capaccioli *et al.* (1990) and Branch & Tammann (1992) that the dust which reddens SNe Ia is characterized by unusually low values of R. Adopting Pierce's Tully–Fisher distance to NGC 3627, and assuming a total reddening of $E(B-V)=0.37\pm0.03$ mags for SN 1989B, we derive extinction-corrected absolute magnitudes of $M_B=-18.58\pm0.33$ and $M_V=-18.56\pm0.32$. These are in excellent agreement with the absolute magnitudes for SN 1980N, $M_B=-18.53\pm0.15$ and $M_V=-18.58\pm0.14$, derived from the SBF distance to NGC 1316 (Phillips 1993).

5. CONCLUSIONS

We have presented extensive optical photometry and spectroscopy of the Type Ia SN 1989B. In virtually all respects, this supernova appears to have been a typical representative of the Ia class. The spectroscopic observations, which provide the most detailed look yet of the evolution of a SN Ia, show that the transition to a spectrum dominated by blends of Fe-peak element emission lines occurred around 10–12 days after B maximum. The transition to the "nebular phase" where lines of [Fe II], [Fe III], and [Co III] prevail took place much more gradually between days 80–100. SN 1989B appears to have been significantly reddened. From a comparison of the *UBVRIJHK* light curves with comparable data for the unobscured Type Ia SN 1980N, we obtain a color excess $E(B-V)=0.37\pm0.03$, which is significantly less than previous estimates of the reddening for this supernova. We derive a distance modulus for SN 1989B relative to SN 1980N of $\Delta\mu=-1.62\pm0.11$, which is in agreement with the relative distances of NGC 3627 (the parent galaxy of SN 1989B) and the Fornax cluster obtained from the Tully–Fisher and surface brightness fluctuation relation. These results provide compelling evidence that the properties of the dust of NGC 3627 responsible for the reddening of SN 1989B were very similar to those of normal dust in the disk of our own Galaxy. In particular, the data do not support an unusually low value of the ratio of total to selective absorption.

L. A. W. gratefully thanks Robert Williams for allocating available DD time to this project. L. A. W. also thanks the KPNO photo lab for their outstanding work. R. P. K. acknowledges the support of NSF Grants Nos. AST-9218475 to Harvard University. J. C. W. acknowledges the support of NSF Grant No. AST-9218035, NASA Grant No. NAGW-2905, and the R. A. Welch Foundation. A. V. F. acknowledges the support of NSF Grants Nos. AST-8957063 and AST-9115174, as well as NSF Cooperative Agreement AST-8809616 (Center for Particle Astrophysics).

REFERENCES

Axelrod, T. S. 1980, Ph.D. thesis, University of California at Santa Cruz
Barbon, R., Benetti, S., Cappellaro, E., Rosino, L., & Turatto, M. 1990, A&A, 237, 79 (BBCRT)
Barbon, R., Cappellaro, E., & Turatto, M. 1989, A&AS, 81, 421
Bolte, M., Saddlemyer, L., Mendes de Oliveira, C., & Hodder, P. 1989, PASP, 101, 921
Branch, D. 1981, ApJ, 248, 1076
Branch, D. 1987, ApJ, 316, L81
Branch, D., Drucker, W., & Jeffery, D. J. 1988, ApJ, 330, L117
Branch, D., Lacy, C. H., McCall, M. L., Sutherland, P. G., Uomoto, A., Wheeler, J. C., & Wills, B. J. 1983, ApJ, 270, 123
Branch, D., & Tammann, G. A. 1992, ARA&A, 30, 359
Burkhead, M. S., & Hutter, D. J., 1981, AJ, 86, 523
Burstein D., & Heiles, C. 1982, ApJS, 54, 33
Capaccioli, M., Cappellaro, E., Della Valle, M., D'Onofrio, M., Rosino, L., & Turatto, M. 1990, ApJ, 350, 110
Cappellaro, E., & Turatto, M. 1989, IAU Circ., No. 4727
Ciatti, F., & Rosino, L. 1977, A&A, 56, 59
Doggett, J. B., & Branch, D. 1985, AJ, 90, 2303
Elias, J. H., Frogel, J. A., Hackwell, J. A., & Persson, S. E. 1981, ApJ, 251, L13
Elias, J. H., Frogel, J. A., Matthews, K., & Neugebauer, G. 1982, AJ, 1029
Elias, J. H., Matthews, K., Neugebauer, G., & Persson, S. E. 1985, ApJ, 296, 379
Evans, R. O. 1989, IAU Circ., No. 4726
Filippenko, A. V. 1989, IAU Circ., No. 4728
Filippenko, A. V., *et al.* 1992a, ApJ, 384, L15
Filippenko, A. V., *et al.* 1992b, AJ, 104, 1543

Ford, C. H., Herbst, W., Richmond, M. W., Baker, M. L., Filippenko, A. V., Treffers, R. R., Paik, Y., & Benson, P. J. 1993, AJ, 106, 1101
Graham, J. A. 1982, PASP, 94, 244
Hamuy, M., Phillips, M. M., Maza, J., Wischnjewsky, M., Uomoto, A., Landolt, A., & Khatwani, R. 1991, AJ, 102, 208
Harkness, R. P. 1991, in ESO/EIPC Workshop, SN 1987A and other Supernovae, edited by I. J. Danziger and K. Kjär (ESO, Garching), p. 447
Herbig, G. 1975, ApJ, 196, 129
Höflich, P., Khoklov, A., & Müller 1991, A&A, 248, L7
Jeffery, D. J., Leibundgut, B., Kirshner, R. P., Benetti, S., Branch, D., & Sonneborn, G. 1992, ApJ, 397, 304
Kirshner, R. 1989, IAU Circ., No. 4727
Kirshner, R., Oke, J. B., Penston, M. V., & Searle, L. 1973, ApJ, 185, 303
Kuchner, M. J., Kirshner, R. P., Pinto, P. A., & Leibundgut, B. 1994, ApJ, 426, L89
Landolt, A. U. 1983, AJ, 88, 439
Leibundgut, B. 1988, thesis, Universitat Basel
Leibundgut, B., Kirshner, R. P., Filippenko, A. V., Shields, J. C., Foltz, C. B., Phillips, M. M., & Sonneborn, G. 1991, ApJ, 371, L23
Leibundgut, B., *et al.* 1993, AJ, 105, 301
Lynch, D. K., Rudy, R. J., Rossano, G. S., Erwin, P., Puetter, R. C., & Branch, D. 1990, AJ, 100, 223
Marvin, H., & Perlmutter, S. 1989, IAU Circ., No. 4727
Massey, P. Strobel, K., Barnes, J. V., & Anderson, E. 1988, ApJ, 328, 315
Minkowski, R. 1939, ApJ, 89, 143
Oke, J. B., & Gunn, J. E. 1983, ApJ, 266, 713
Phillips, M. M. 1993, ApJ, 413, L105
Phillips, M. M., *et al.* 1987, PASP, 99, 592
Phillips, M. M., Wells, L. A., Suntzeff, N. B., Hamuy, M., Leibundgut, B., Kirshner, R. P., & Foltz, C. B. 1992, AJ, 103, 1632
Pierce, M. J. 1994, ApJ (in press)
Prabhu, T. P., & Krishnamurthi, A. 1990, A&A, 232, 75
Pskovskii, Y. P. 1967, SovA, 11, 63
Pskovskii, Y. P. 1977, SovA, 21, 675
Pskovskii, Y. P. 1984, SovA, 28, 658
Sandage, A., & Tammann, G. 1981, A Revised Shapley-Ames Catalog of Bright Galaxies (Carnegie Institution of Washington, Washington, DC)
Savage, B. D., & Mathis, J. S. 1979, ARA&A, 17, 73
Schechter, P. L., Mateo, M., & Saha, A. 1993, PASP, 105, 1342
Spyromilio, J. A., Pinto, P., & Eastman, R. G. 1994, MNRAS, 266, L17
Stone, R. P. S., & Baldwin, J. A. 1983, MNRAS, 204, 347
Suntzeff, N. 1989, IAU Circ., No. 4728
Suntzeff, N. 1994, in preparation
Tonry, J. L. 1994, in preparation
Tsvetkov, D. Yu., Kimeridze, G. N., Volkov, I. M., Bartunov, O. S., & Ikonnikova, N. P. 1990, A&A, 236, 133 (TKVBI)
Volkov, I. M. 1991, Information Bulletin on Variable Stars, No. 3581

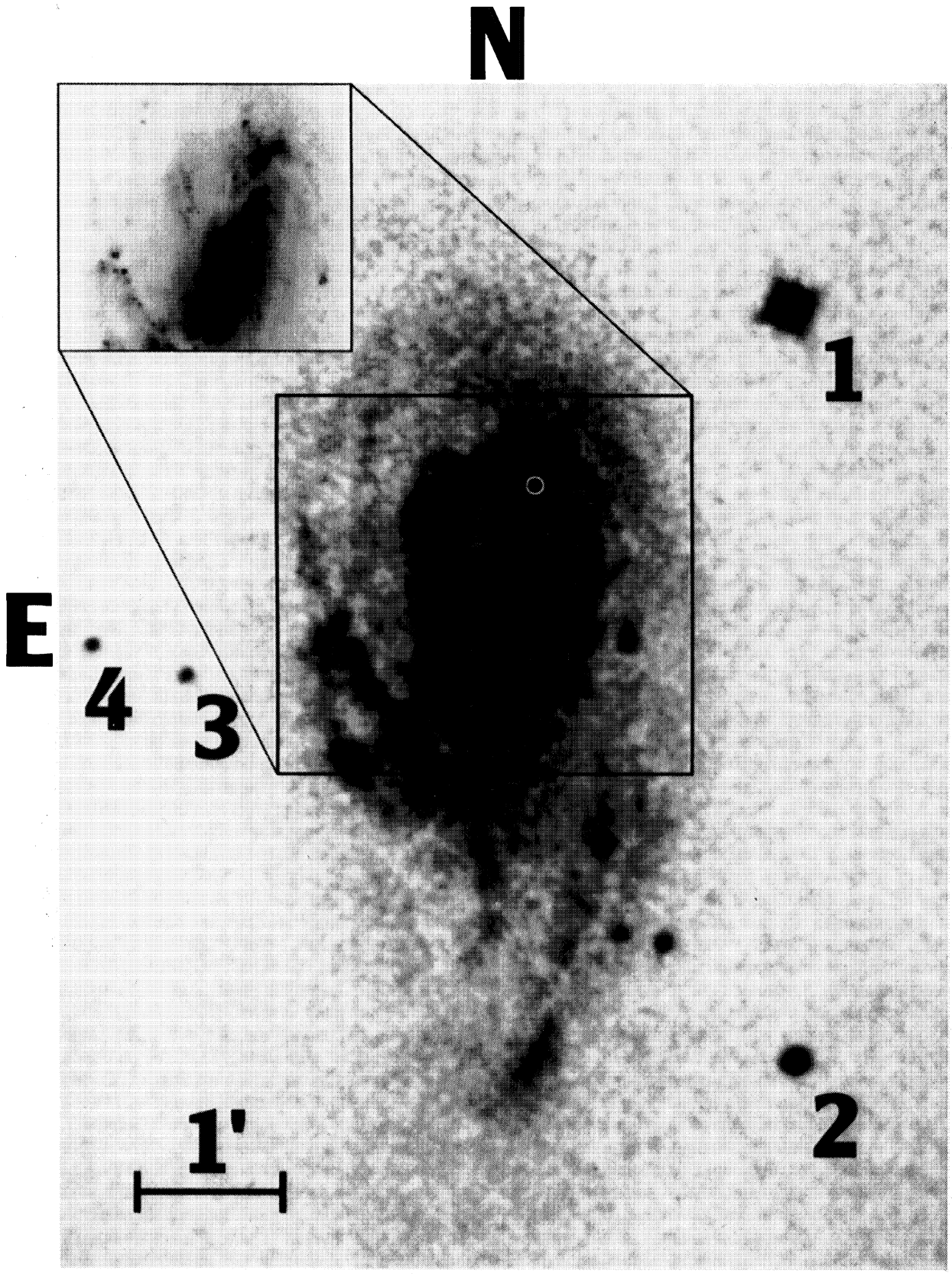

FIG. 1. The photograph of NGC 3627 from a 103aO emulsion plate taken with the CTIO Curtis Schmidt telescope indicates the position of SN 1989B and the local calibration standards labeled corresponding to the magnitudes listed in Table 2. The inset is the central region of a *V* band image taken at the CTIO 0.9 m telescope near maximum.